

Supporting Information

**Aluminum Complexes with Bidentate Amido Ligands:  
Synthesis, Structure and Performance on  
Ligand-Initiated Ring-Opening Polymerization of  
*rac*-Lactide**

Junpeng Liu and Haiyan Ma\*

Shanghai Key Laboratory of Functional Materials Chemistry and Laboratory of Organometallic  
Chemistry, East China University of Science and Technology, Shanghai 200237, P. R. China.

\* Email: [haiyanma@ecust.edu.cn](mailto:haiyanma@ecust.edu.cn); Tel. 021-64253519

## 1. X-ray diffraction data of complexes 2b and 3b.

**Table S1. The crystal data and structure refinement for complexes 2b and 3b.**

	<b>2b</b>	<b>3b</b>
Formula	C <sub>23</sub> H <sub>35</sub> AlN <sub>2</sub>	C <sub>22</sub> H <sub>31</sub> AlN <sub>2</sub>
Formula weight	366.51	350.47
Temperature (K)	293(2)	293(2)
Crystal system	Monoclinic	Orthorhombic
Space group	P 21/c	P 21 21 21
<i>a</i> (Å)	10.075(3)	7.880(3)
<i>b</i> (Å)	17.439(6)	13.970(5)
<i>c</i> (Å)	13.495(5)	18.482(7)
$\alpha$ (°)	90	90
$\beta$ (°)	105.666(4)	90
$\gamma$ (°)	90	90
<i>V</i> (Å <sup>3</sup> )	2283.0(13)	2034.5(14)
<i>Z</i>	4	4
Density (g·cm <sup>-3</sup> )	1.066	1.144
Absorp coeff/mm <sup>-1</sup>	0.097	0.106
<i>F</i> (000)	800	760
Data collected (hkl)	-12 ≤ <i>h</i> ≤ 12, -21 ≤ <i>k</i> ≤ 11, -16 ≤ <i>l</i> ≤ 16	-9 ≤ <i>h</i> ≤ 10, -16 ≤ <i>k</i> ≤ 17, -22 ≤ <i>l</i> ≤ 23
$\theta$ range for data collection/°	1.954 to 26.010	1.827 to 27.010
Max. and min. transmission	1 and 0.753	1 and 0.507
Data/restraints/parameters	4494 / 0 / 239	4339 / 0 / 230
Goodness-of-fit on <i>F</i> <sup>2</sup>	0.902	0.936
Final <i>R</i> indices [ <i>I</i> > 2σ( <i>I</i> )]	<i>R</i> 1 = 0.0453, <i>wR</i> 2 = 0.1140	<i>R</i> 1 = 0.0389, <i>wR</i> 2 = 0.0919
<i>R</i> indices (all data)	<i>R</i> 1 = 0.0898, <i>wR</i> 2 = 0.1287	<i>R</i> 1 = 0.0518, <i>wR</i> 2 = 0.0972
Largest diff. peak and hole/e Å <sup>-3</sup>	0.261 and -0.192	0.163 and -0.166

2.  $^1\text{H}$  NMR and  $^{13}\text{C}$  NMR spectra of proligands 1a-1j and aluminum complexes 2b, 2d, 3a-3j.

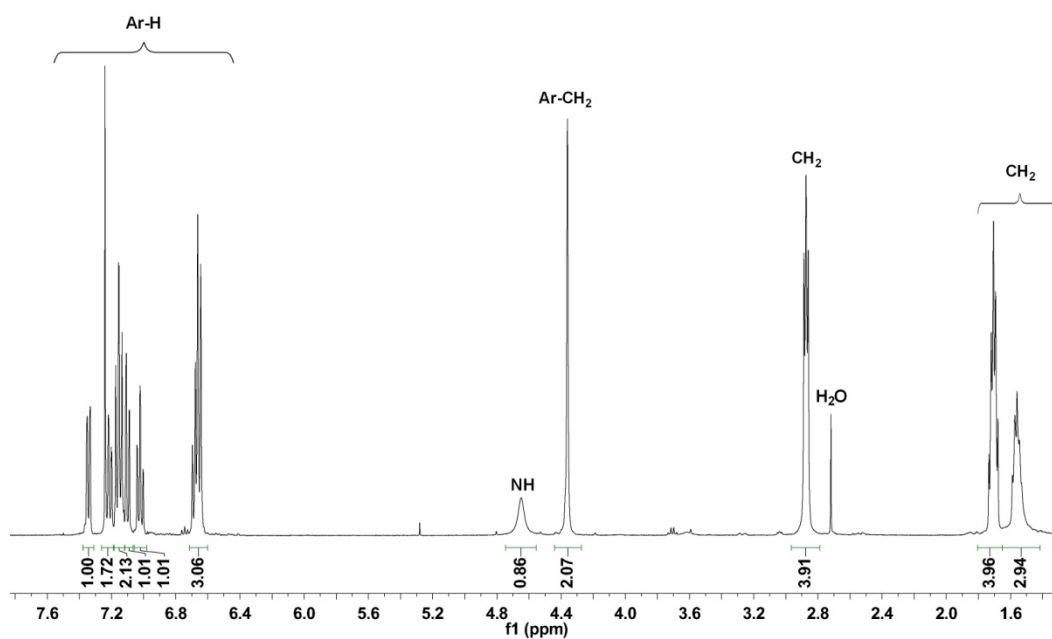


Figure S1. The  $^1\text{H}$  NMR spectrum of compound **1a** ( $\text{CDCl}_3$ , 400 MHz).

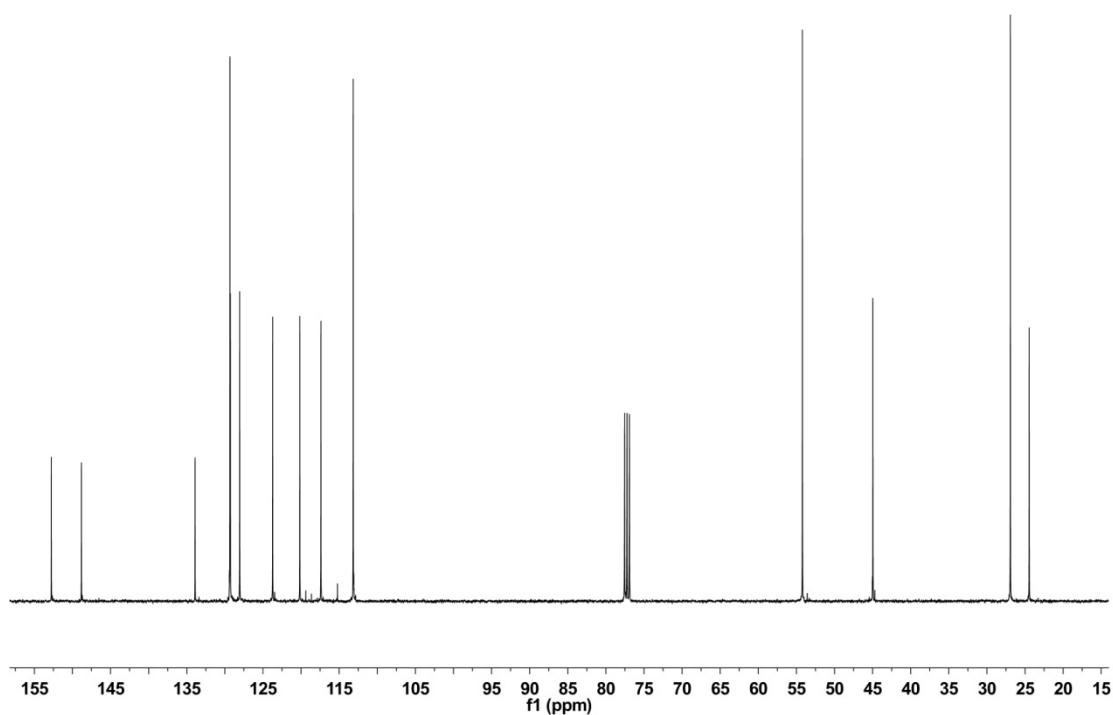
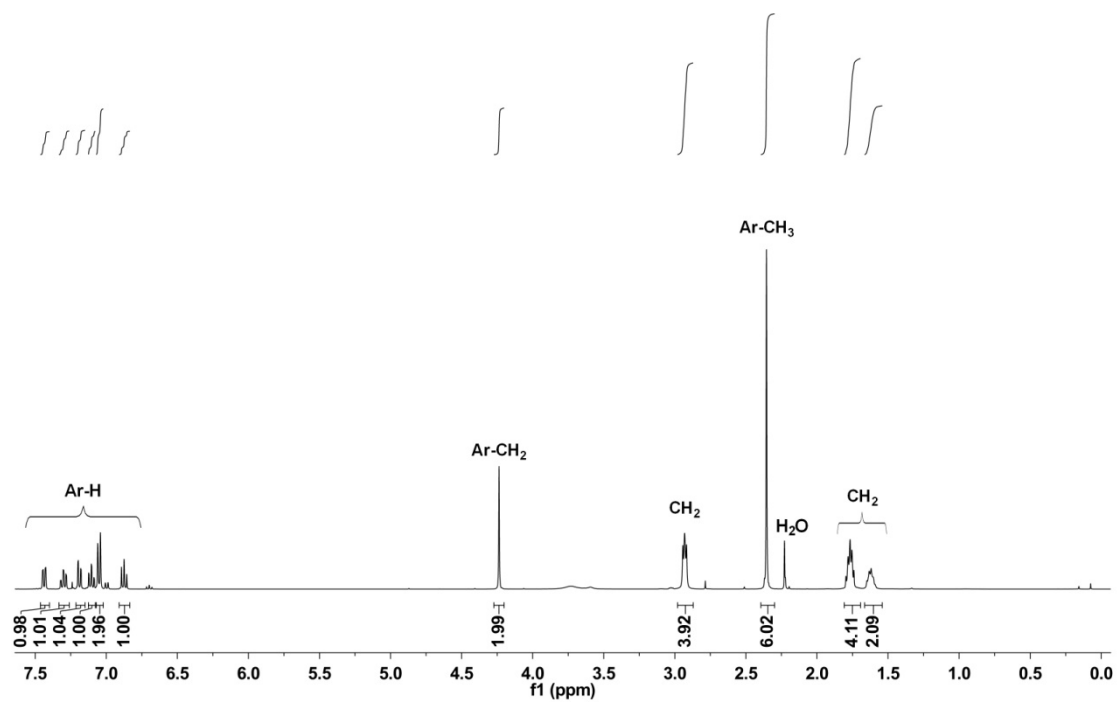
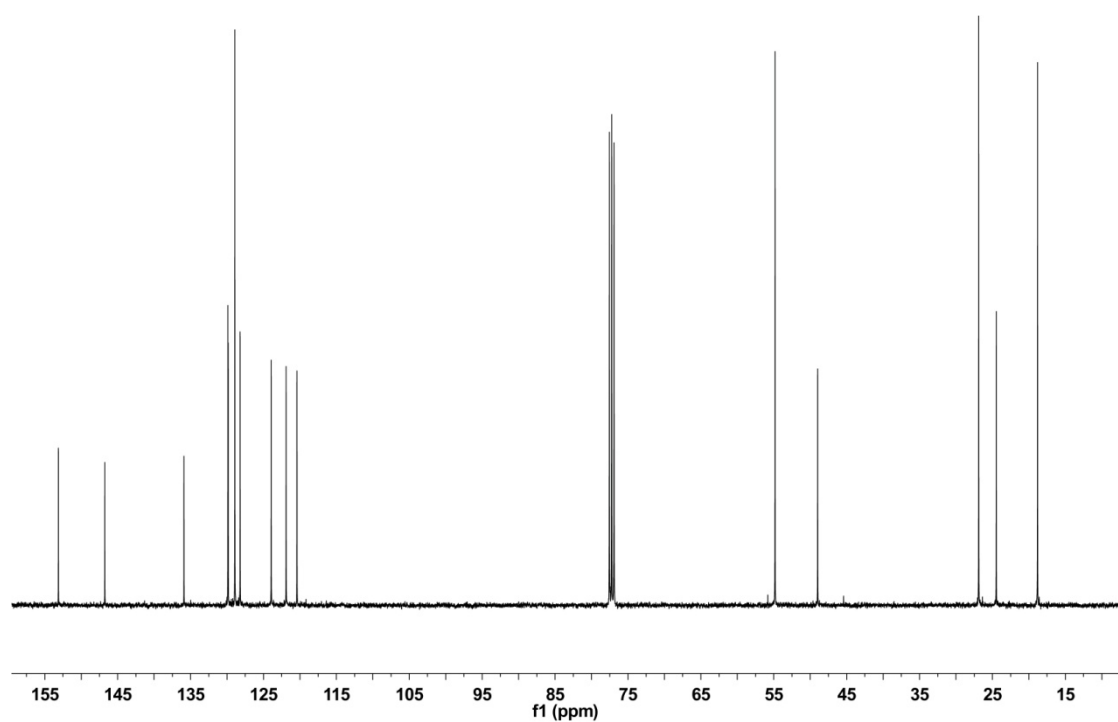


Figure S2. The  $^{13}\text{C}$  NMR spectrum of compound **1a** ( $\text{CDCl}_3$ , 100 MHz).



**Figure S3.** The  $^1\text{H}$  NMR spectrum of compound **1b** ( $\text{CDCl}_3$ , 400 MHz).



**Figure S4.** The  $^{13}\text{C}$  NMR spectrum of compound **1b** ( $\text{CDCl}_3$ , 100 MHz).

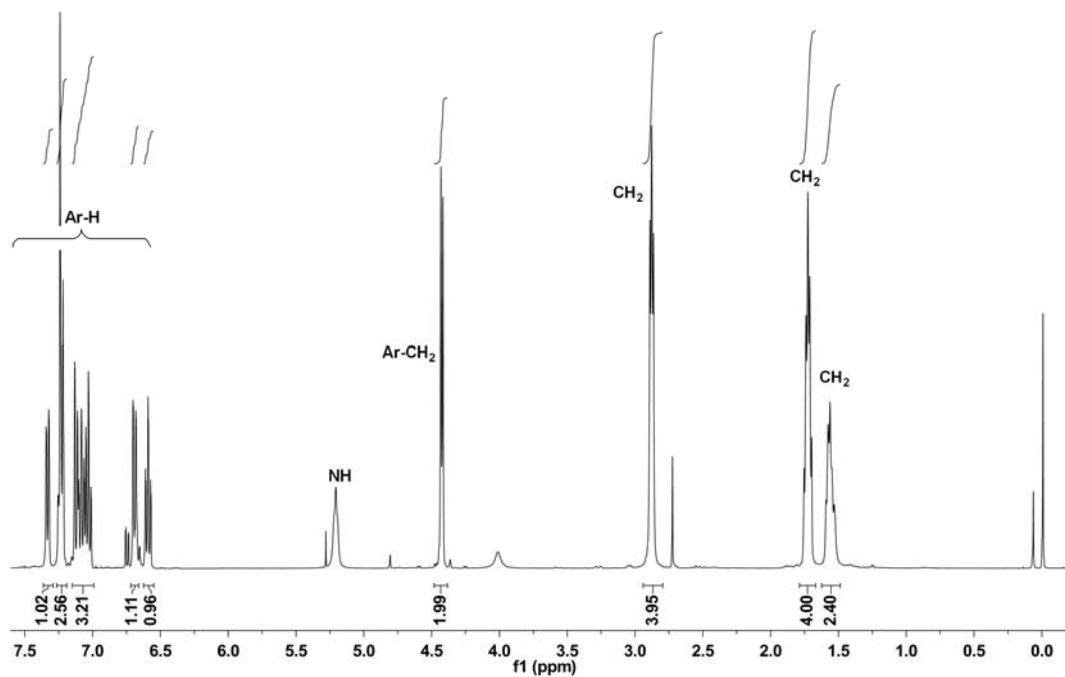


**Figure S5.** The  $^1\text{H}$  NMR spectrum of compound **1c** ( $\text{CDCl}_3$ , 400 MHz).

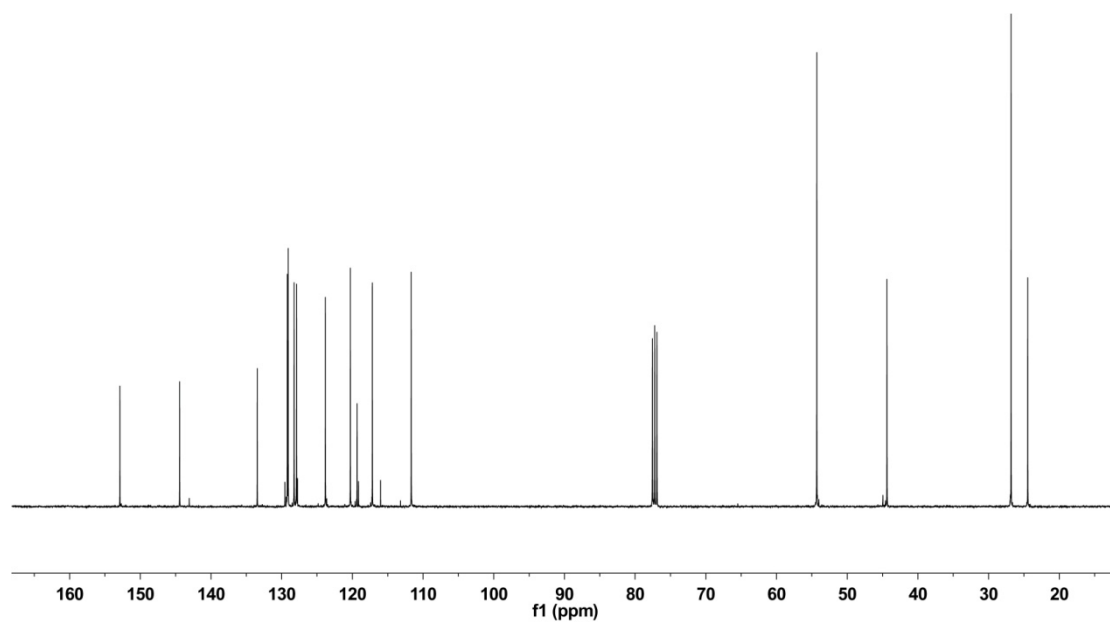


**Figure S6.** The  $^{13}\text{C}$  NMR spectrum of compound **1c** ( $\text{CDCl}_3$ , 100 MHz).

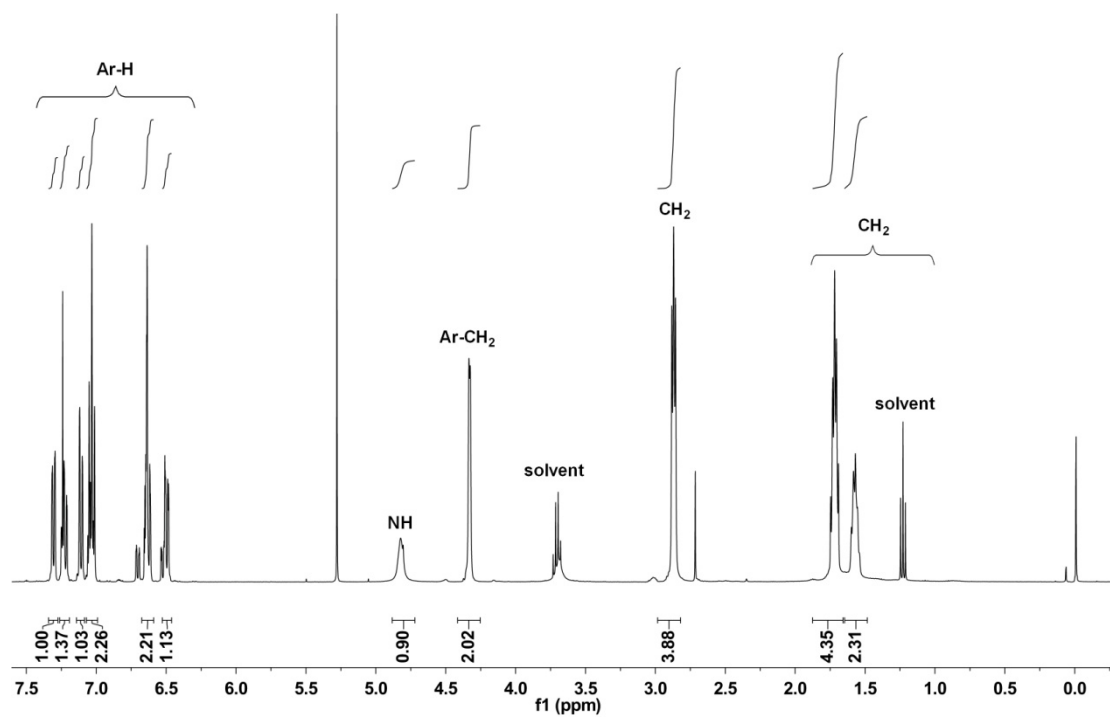


**Figure S7.** The  $^1\text{H}$  NMR spectrum of compound **1d** ( $\text{CDCl}_3$ , 400 MHz).

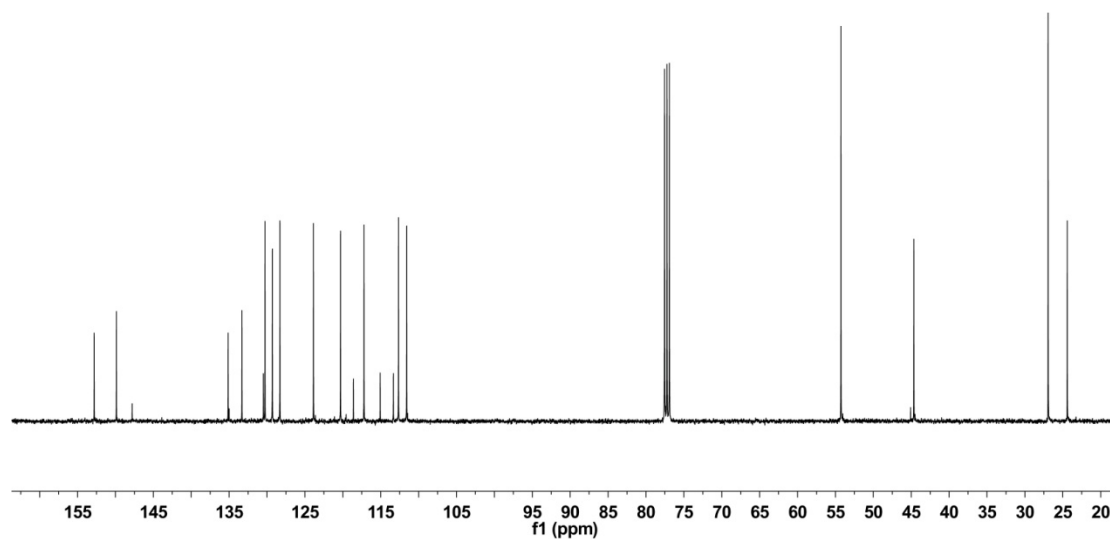


**Figure S8.** The  $^{13}\text{C}$  NMR spectrum of compound **1d** ( $\text{CDCl}_3$ , 100 MHz).

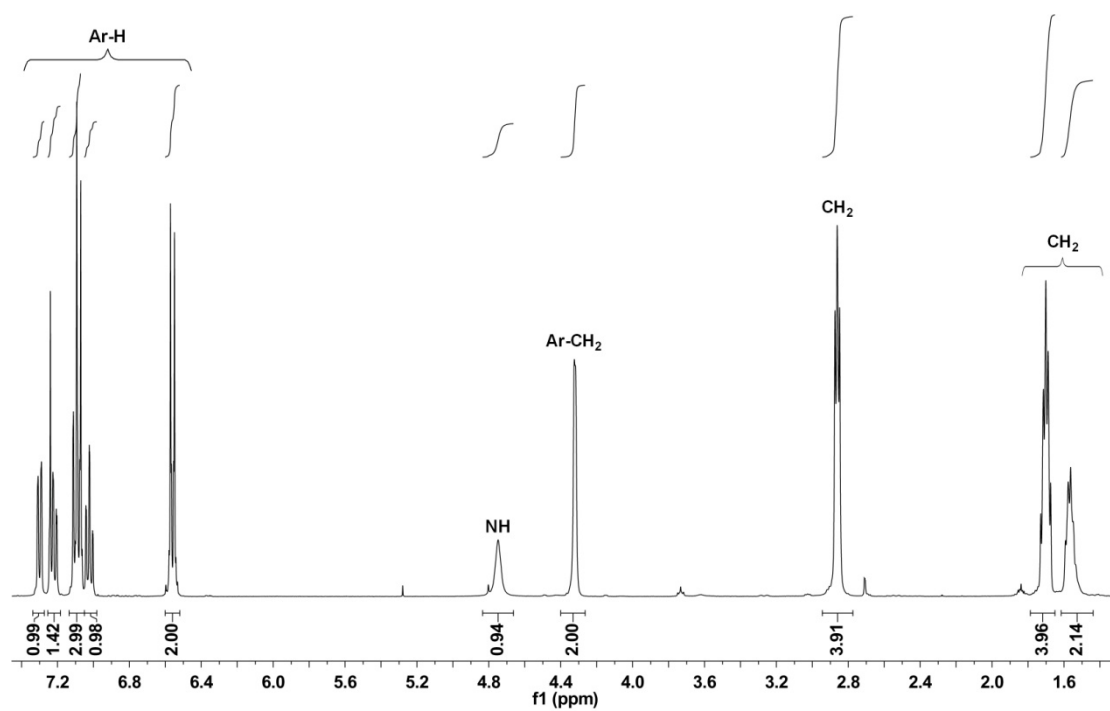


**Figure S9.** The  $^1\text{H}$  NMR spectrum of compound **1e** ( $\text{CDCl}_3$ , 400 MHz).

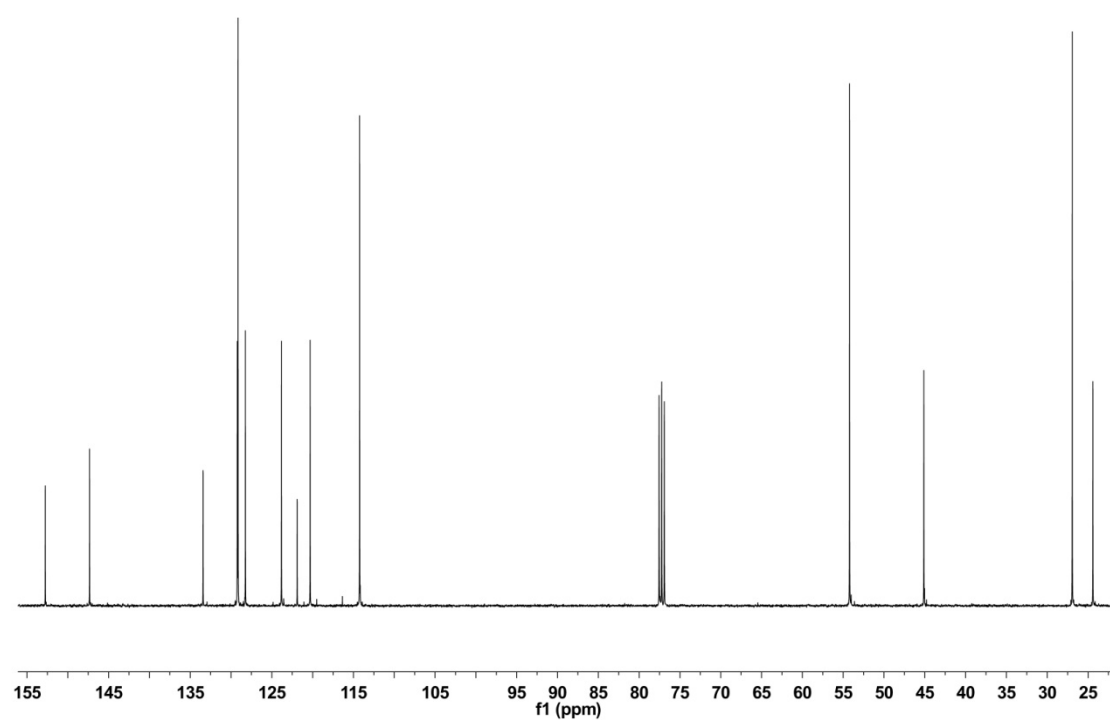


**Figure S10.** The  $^{13}\text{C}$  NMR spectrum of compound **1e** ( $\text{CDCl}_3$ , 100 MHz).

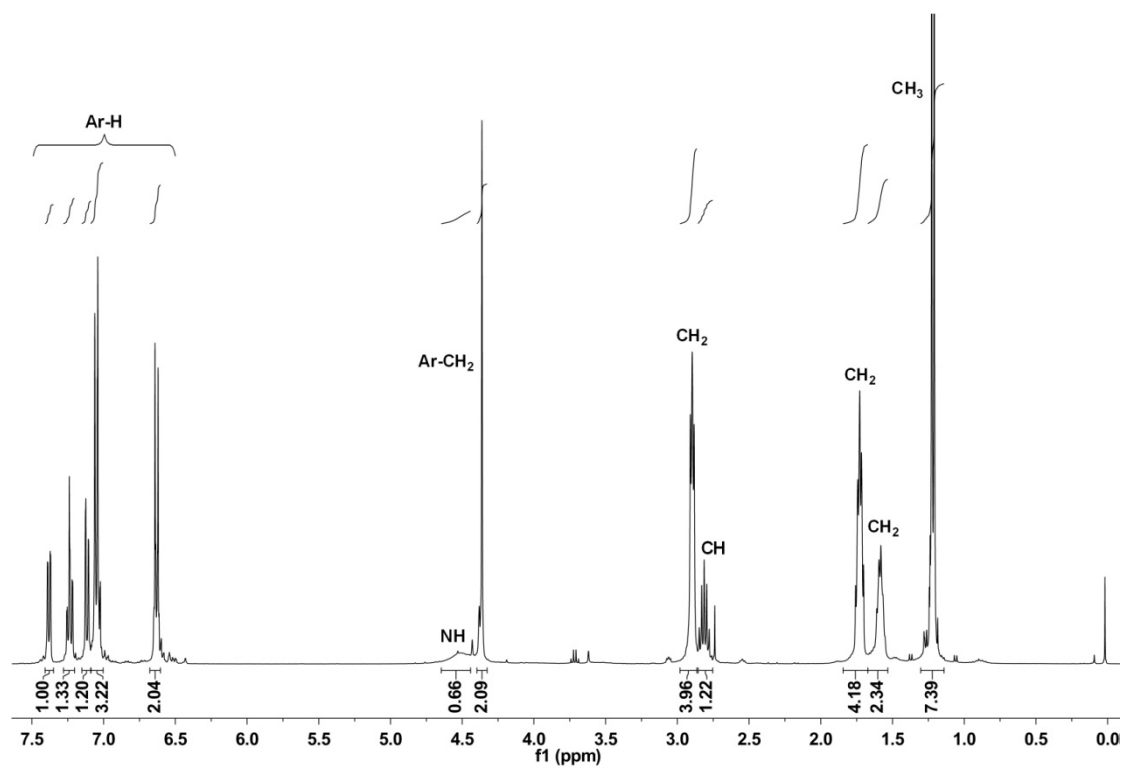


**Figure S11.** The  $^1\text{H}$  NMR spectrum of compound **1f** ( $\text{CDCl}_3$ , 400 MHz).

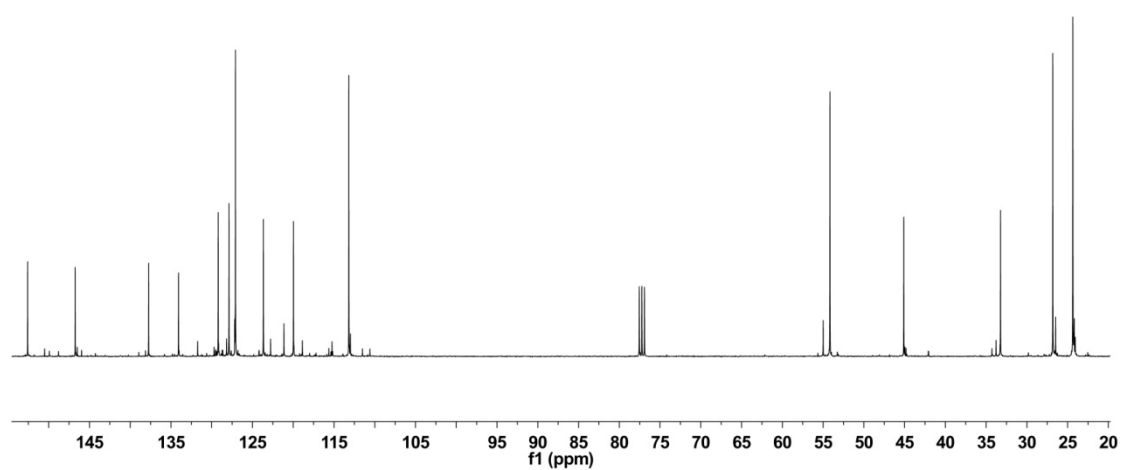


**Figure S12.** The  $^{13}\text{C}$  NMR spectrum of compound **1f** ( $\text{CDCl}_3$ , 100 MHz).



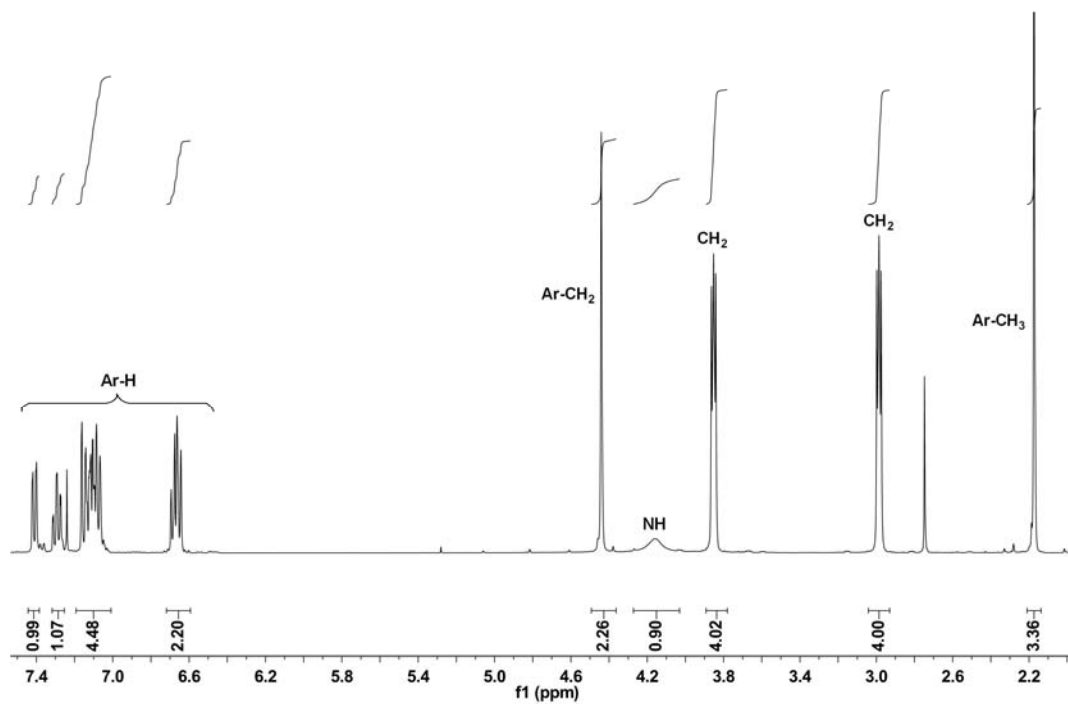


**Figure S13.** The  $^1\text{H}$  NMR spectrum of compound **1g** ( $\text{CDCl}_3$ , 400 MHz).

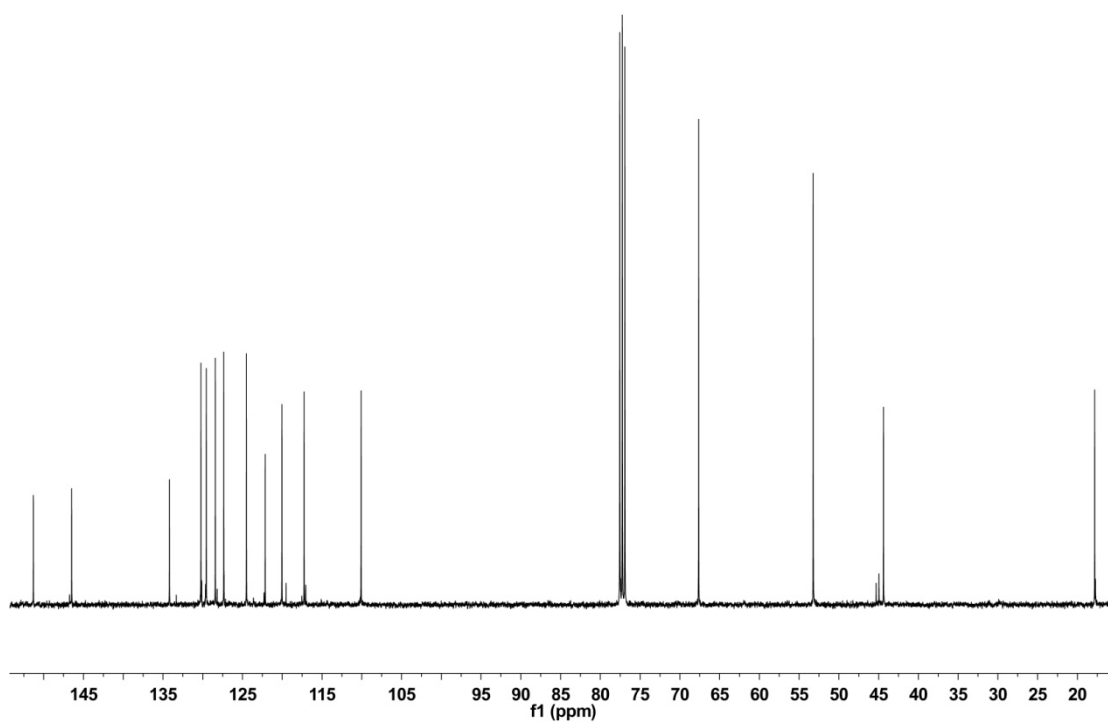


**Figure S14.** The  $^{13}\text{C}$  NMR spectrum of compound **1g** ( $\text{CDCl}_3$ , 100 MHz).

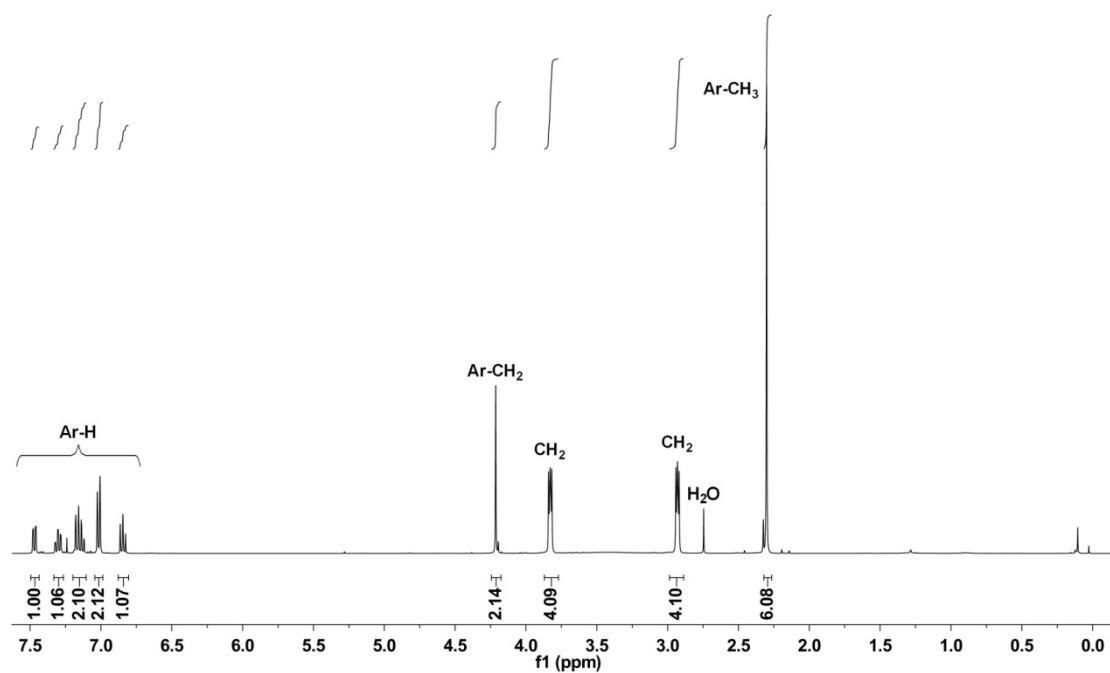


**Figure S15.** The  $^1\text{H}$  NMR spectrum of compound **1h** ( $\text{CDCl}_3$ , 400 MHz).

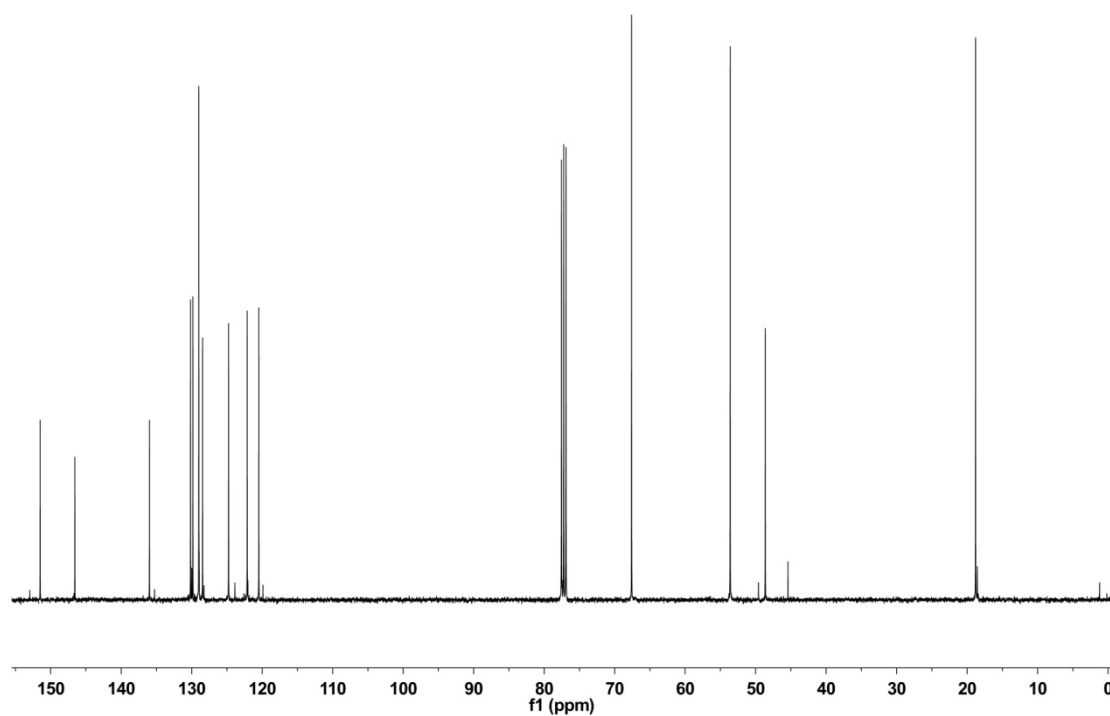


**Figure S16.** The  $^{13}\text{C}$  NMR spectrum of compound **1h** ( $\text{CDCl}_3$ , 100 MHz).

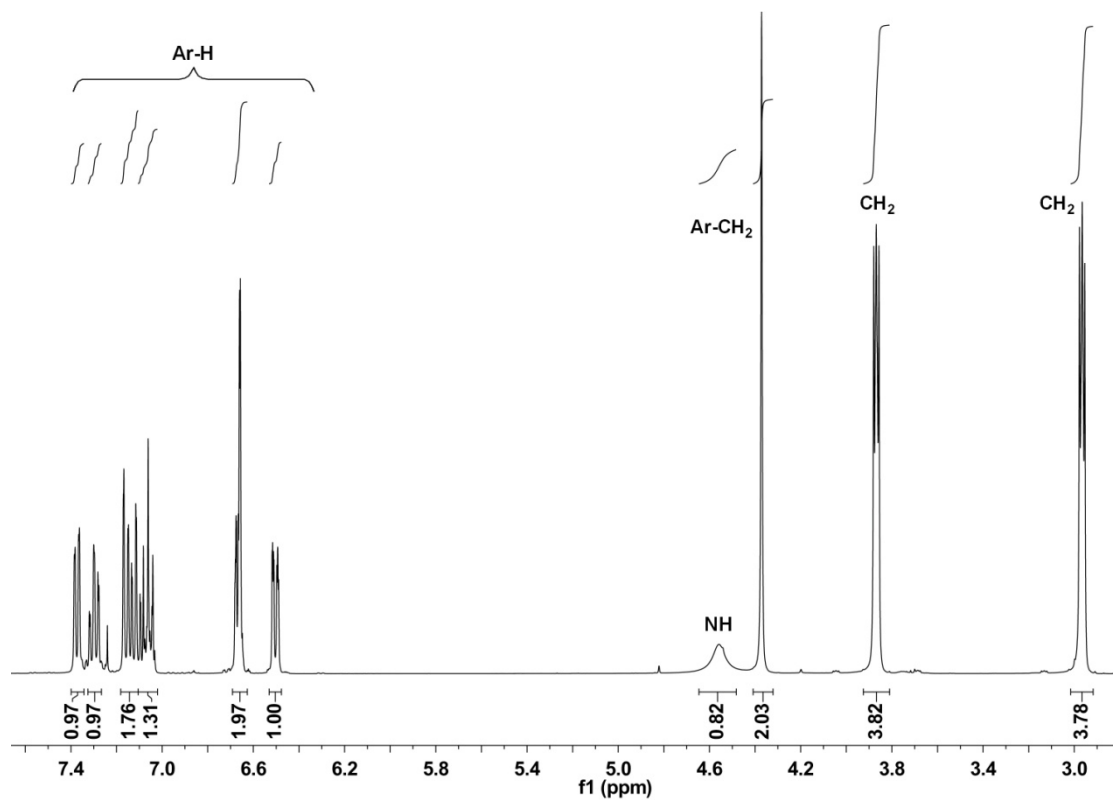


**Figure S17.** The  $^1\text{H}$  NMR spectrum of compound **1i** ( $\text{CDCl}_3$ , 400 MHz).

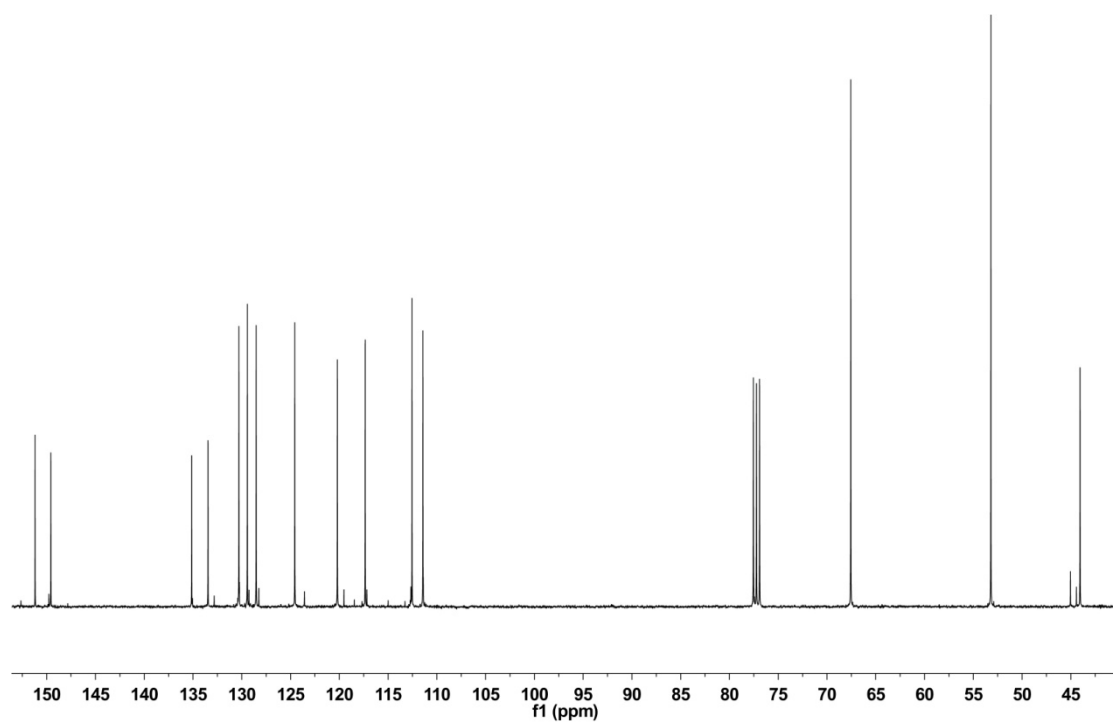


**Figure S18.** The  $^{13}\text{C}$  NMR spectrum of compound **1i** ( $\text{CDCl}_3$ , 100 MHz).

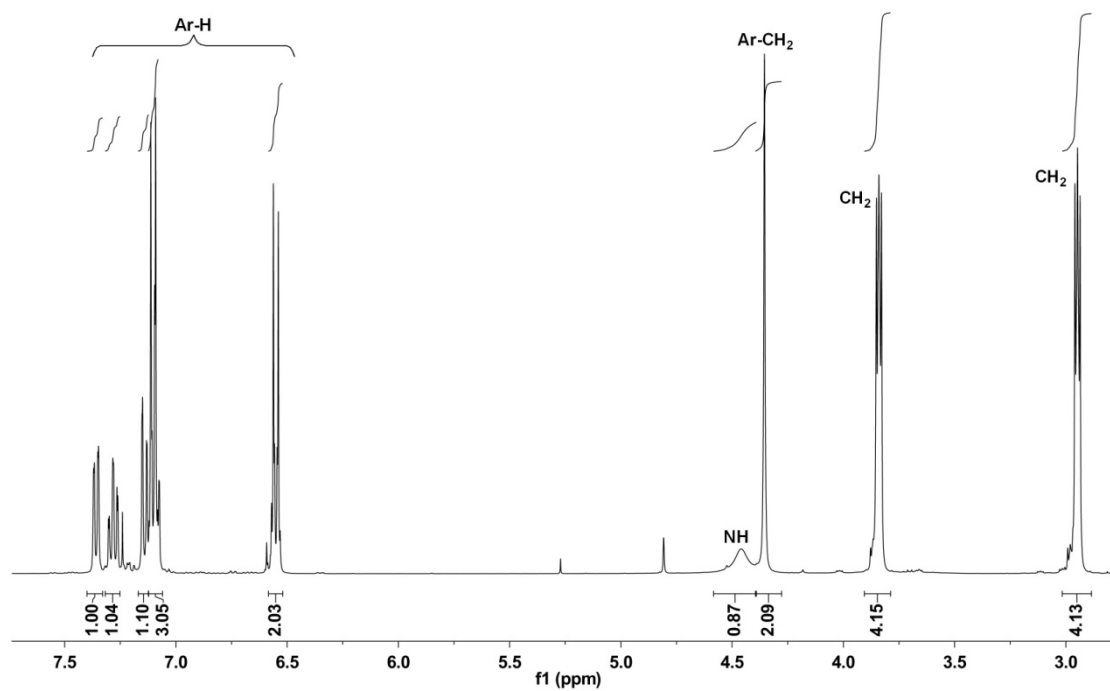


**Figure S19.** The  $^1\text{H}$  NMR spectrum of compound **1j** ( $\text{CDCl}_3$ , 400 MHz).

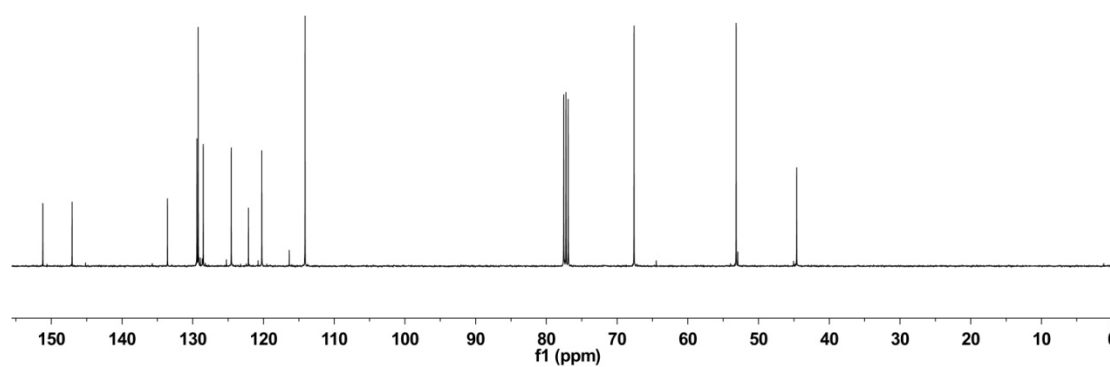


**Figure S20.** The  $^{13}\text{C}$  NMR spectrum of compound **1j** ( $\text{CDCl}_3$ , 100 MHz).

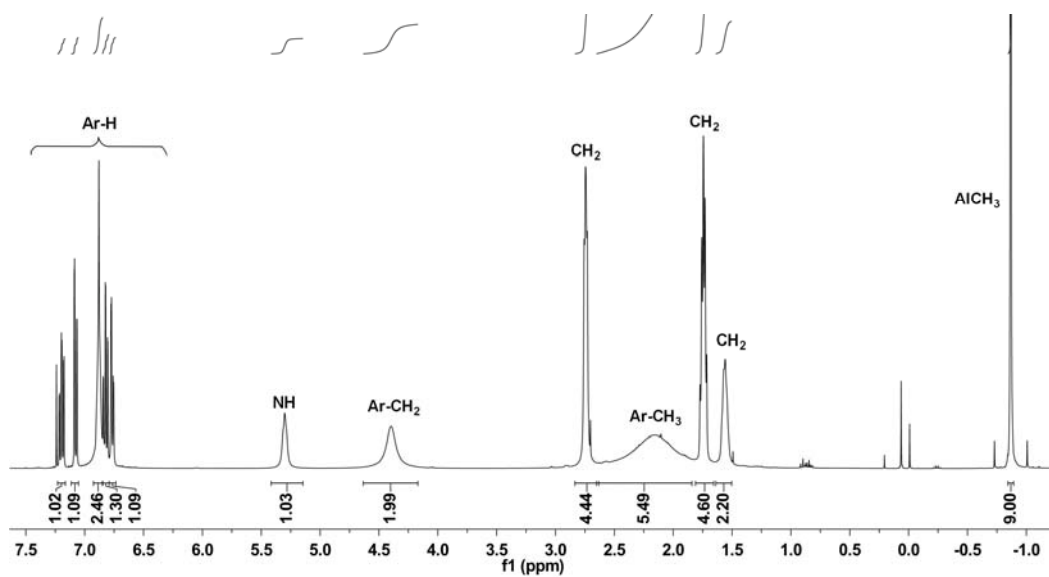


**Figure S21.** The  $^1\text{H}$  NMR spectrum of adduct **2b** ( $\text{CDCl}_3$ , 400 MHz).

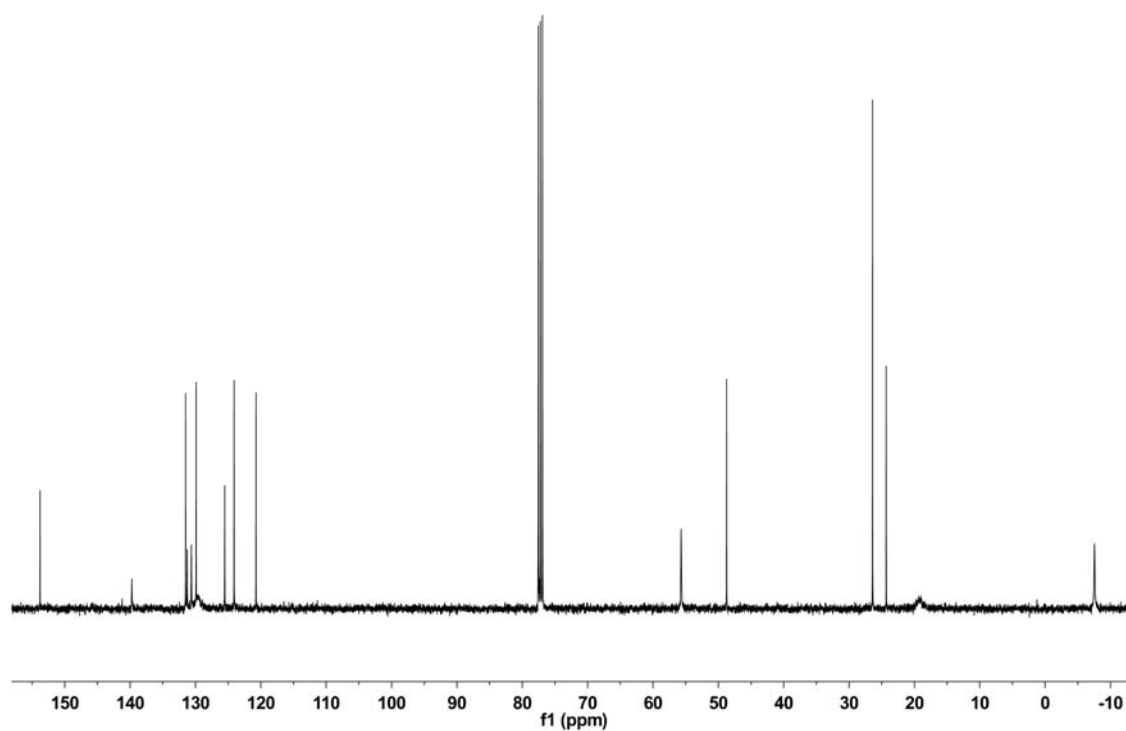


**Figure S22.** The  $^{13}\text{C}$  NMR spectrum of complex **2b** ( $\text{CDCl}_3$ , 100 MHz).

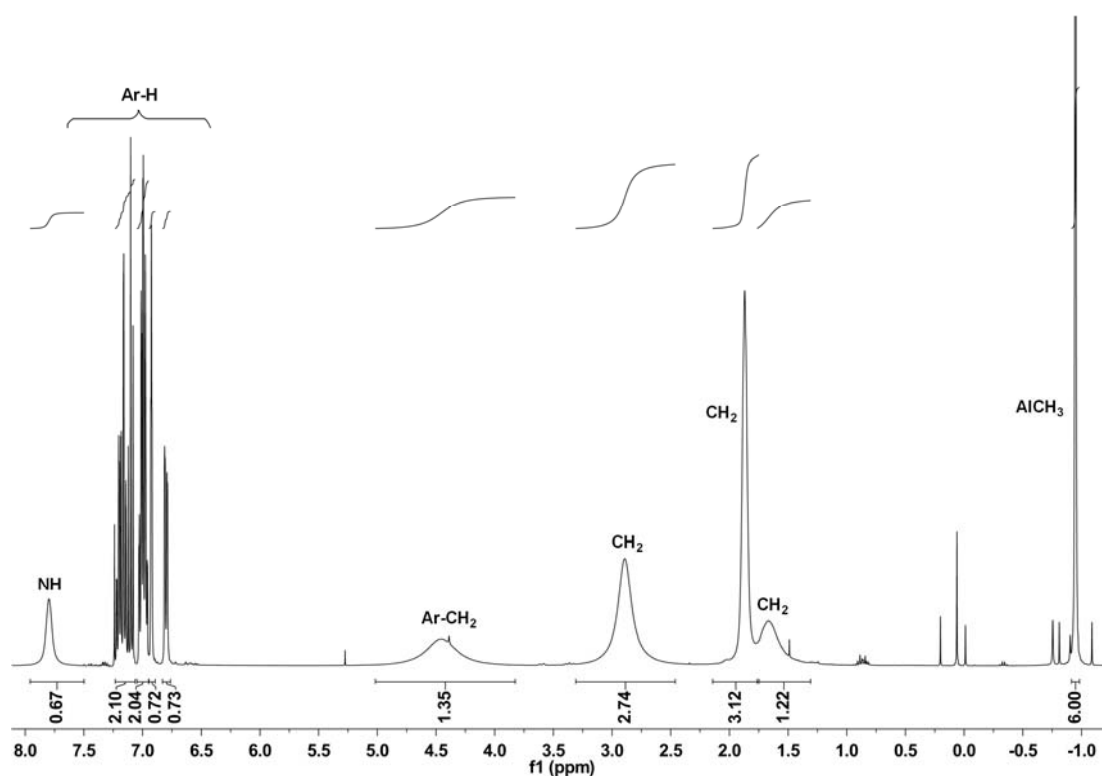


**Figure S23.** The  $^1\text{H}$  NMR spectrum of adduct **2d** ( $\text{CDCl}_3$ , 400 MHz).

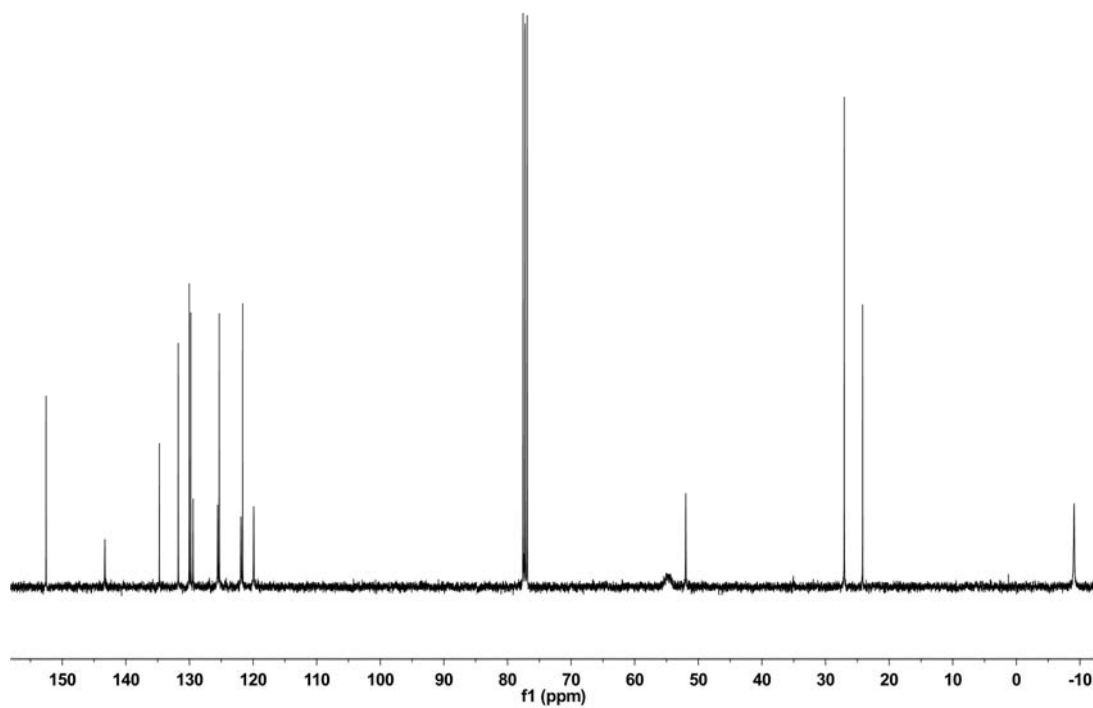


**Figure S24.** The  $^{13}\text{C}$  NMR spectrum of complex **2d** ( $\text{CDCl}_3$ , 100 MHz).

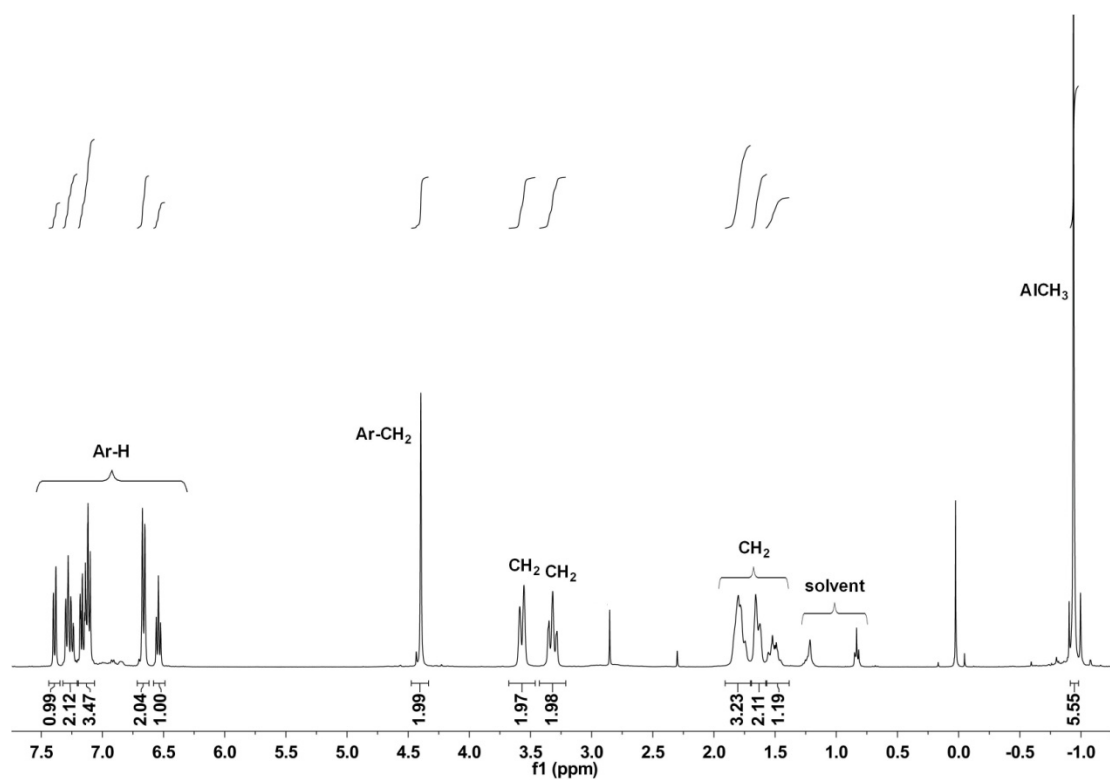


**Figure S25.** The  $^1\text{H}$  NMR spectrum of complex **3a** ( $\text{CDCl}_3$ , 400 MHz).

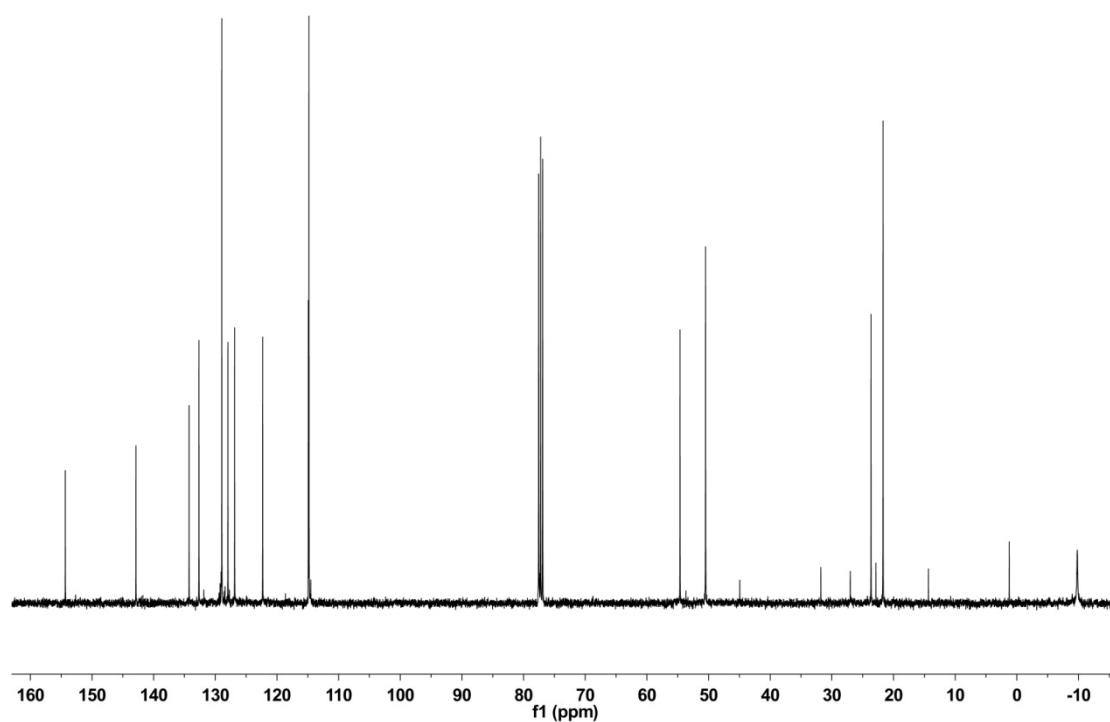


**Figure S26.** The  $^{13}\text{C}$  NMR spectrum of complex **3a** ( $\text{CDCl}_3$ , 100 MHz).

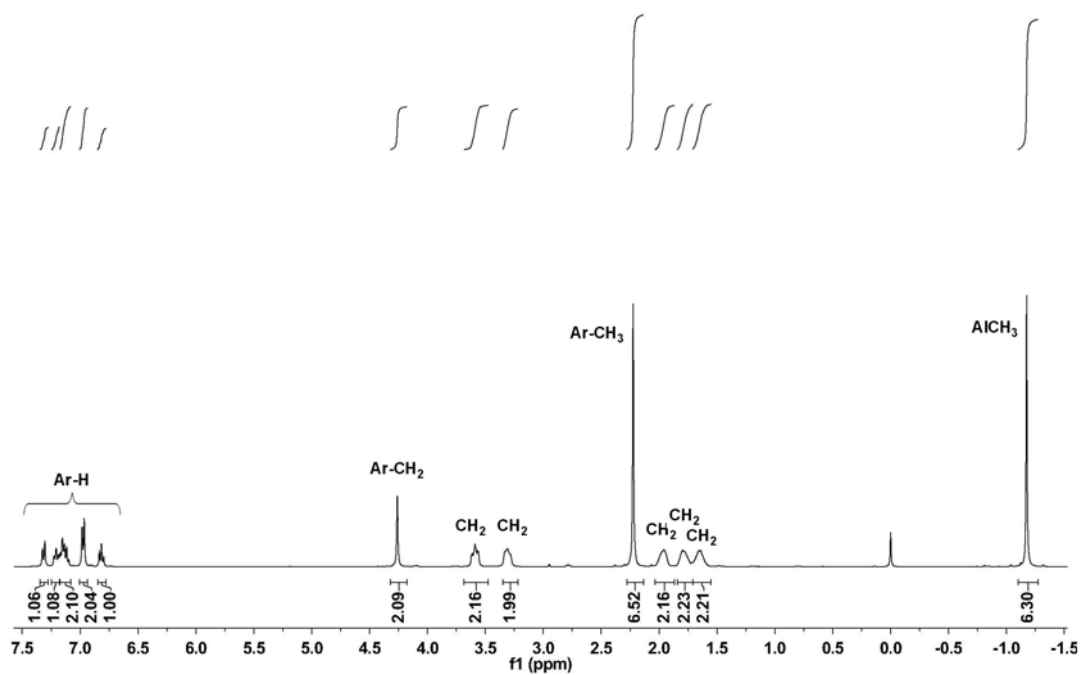


**Figure S27.** The  $^1\text{H}$  NMR spectrum of complex **3b** ( $\text{CDCl}_3$ , 400 MHz).

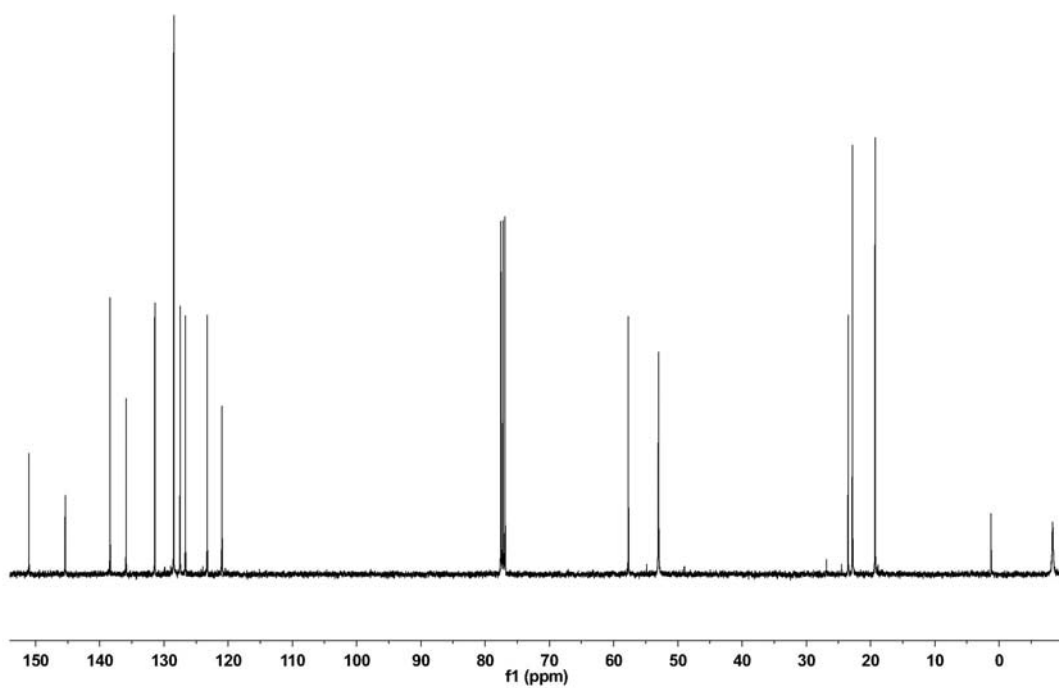


**Figure S28.** The  $^{13}\text{C}$  NMR spectrum of complex **3b** ( $\text{CDCl}_3$ , 100 MHz).



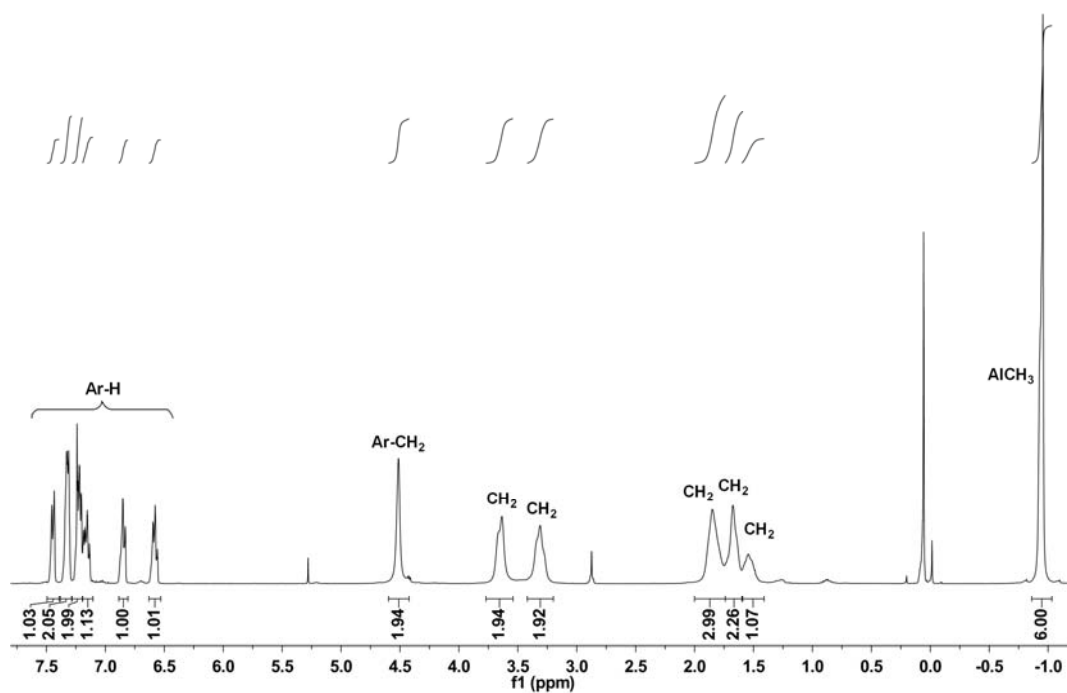


**Figure S29.** The  $^1\text{H}$  NMR spectrum of complex **3c** ( $\text{CDCl}_3$ , 400 MHz).

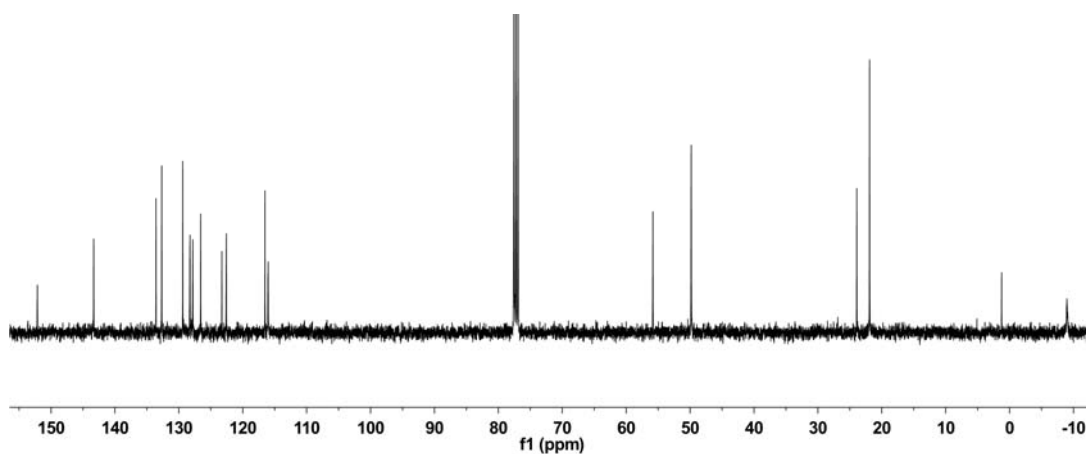


**Figure S30.** The  $^{13}\text{C}$  NMR spectrum of complex **3c** ( $\text{CDCl}_3$ , 100 MHz).

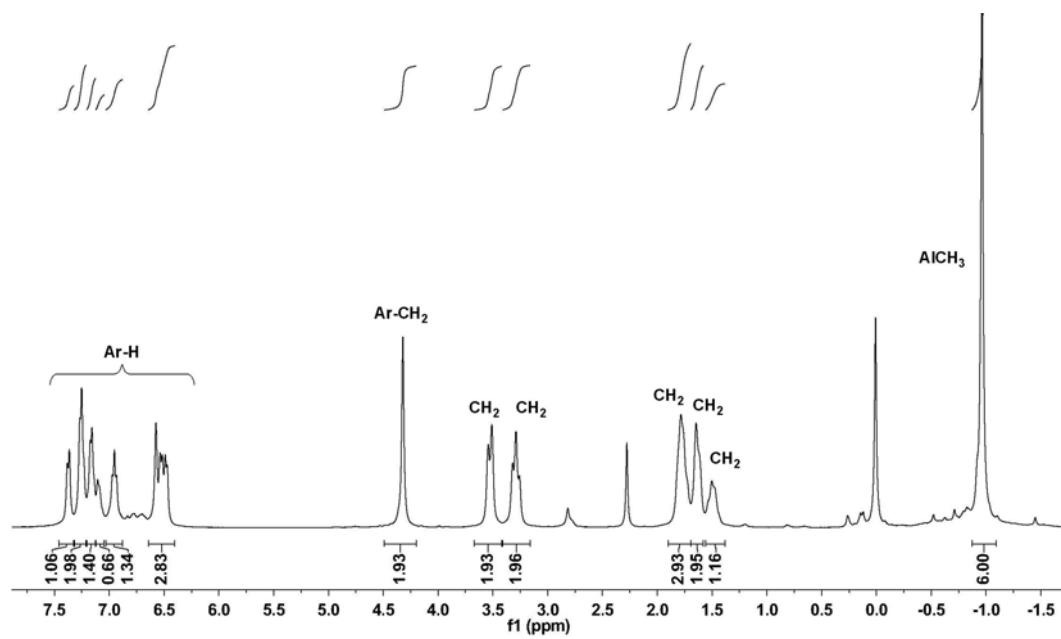


**Figure S31.** The  $^1\text{H}$  NMR spectrum of complex **3d** ( $\text{CDCl}_3$ , 400 MHz).

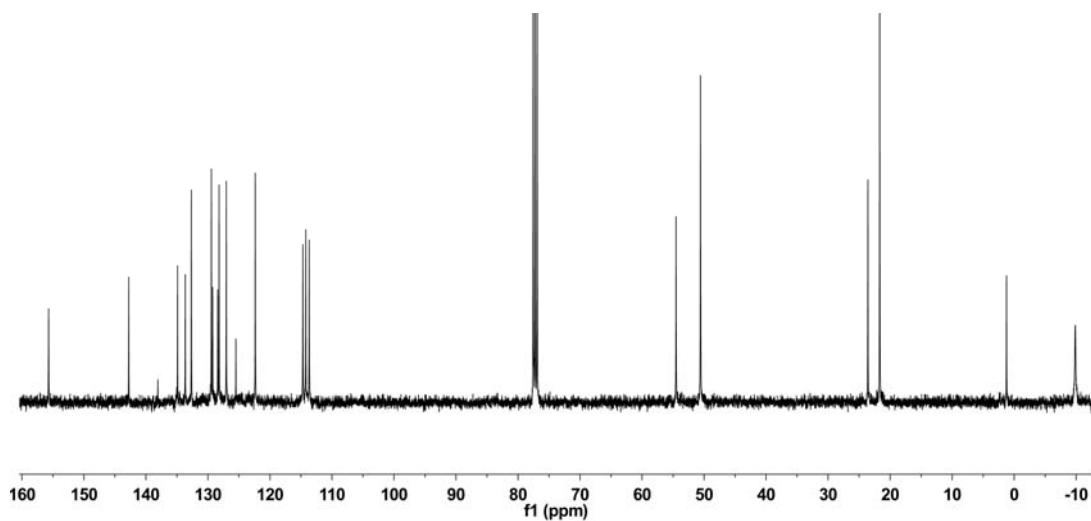


**Figure S32.** The  $^{13}\text{C}$  NMR spectrum of complex **3d** ( $\text{CDCl}_3$ , 100 MHz).

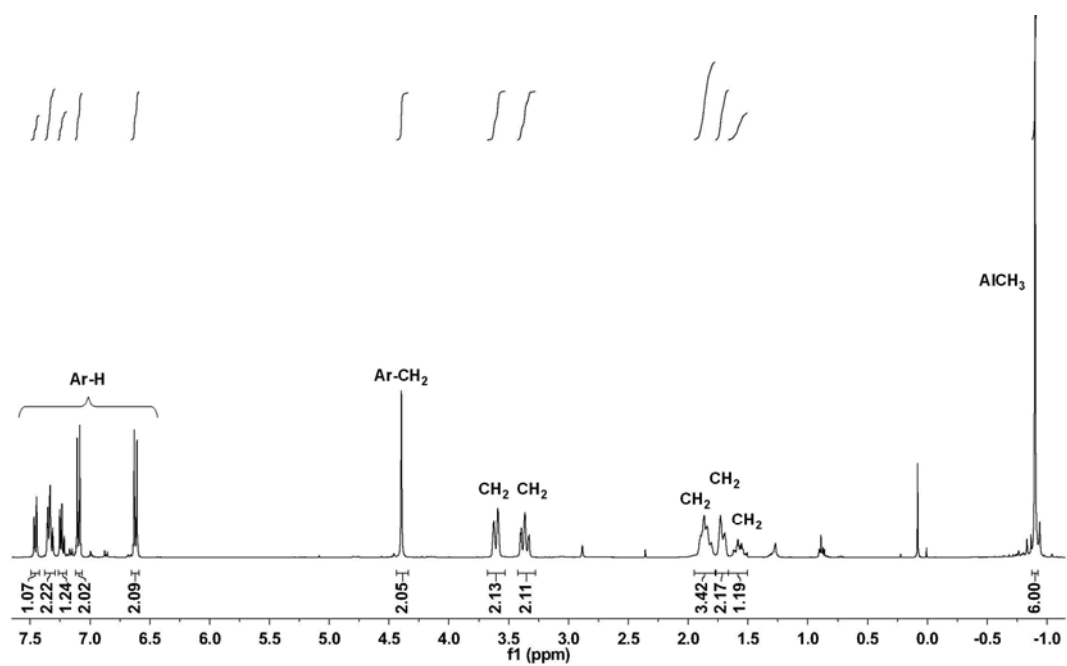


**Figure S33.** The  $^1\text{H}$  NMR spectrum of complex **3e** ( $\text{CDCl}_3$ , 400 MHz)

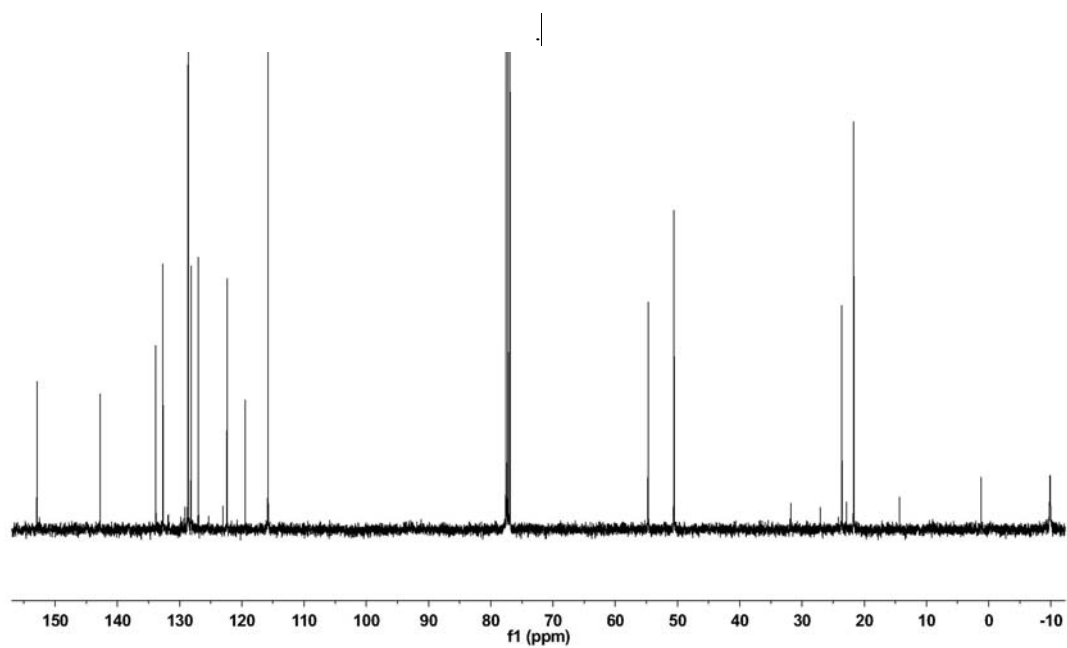


**Figure S34.** The  $^{13}\text{C}$  NMR spectrum of complex **3e** ( $\text{CDCl}_3$ , 100 MHz).

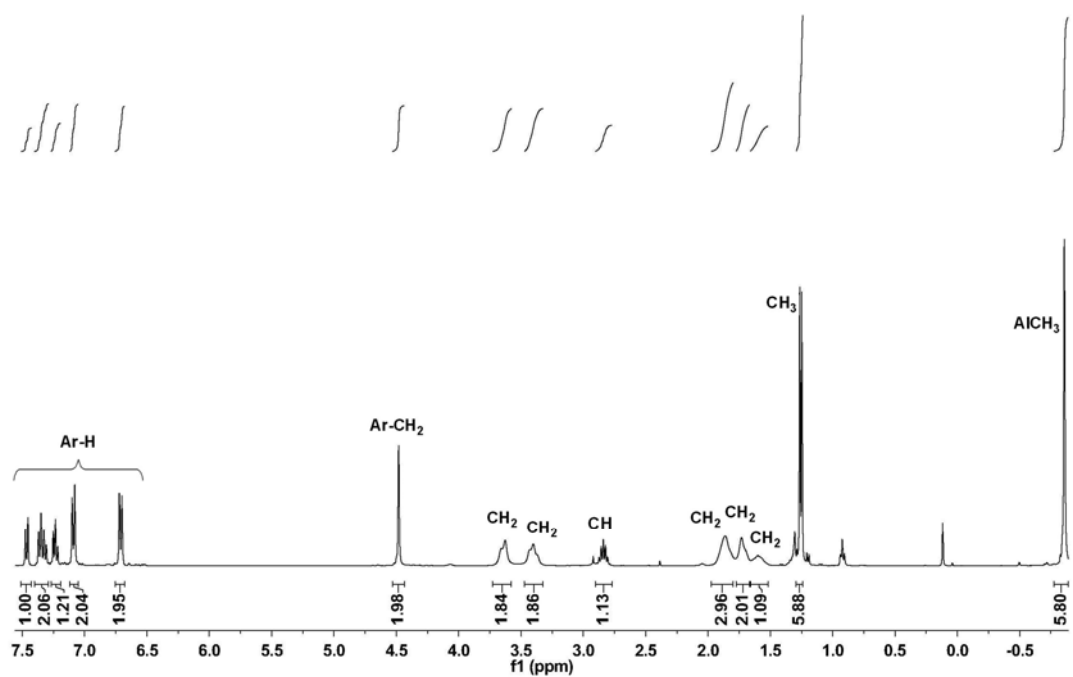


**Figure S35.** The  $^1\text{H}$  NMR spectrum of complex **3f** ( $\text{CDCl}_3$ , 400 MHz).

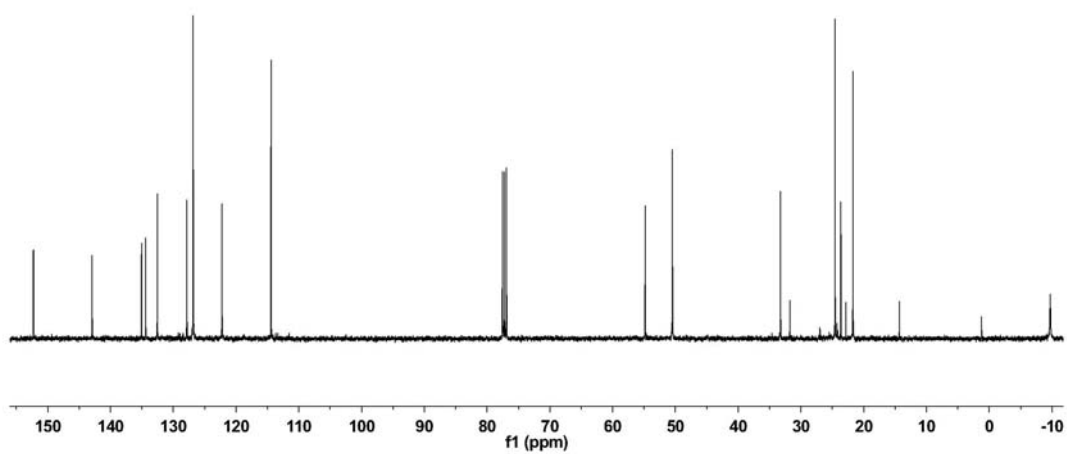


**Figure S36.** The  $^{13}\text{C}$  NMR spectrum of complex **3f** ( $\text{CDCl}_3$ , 100 MHz).

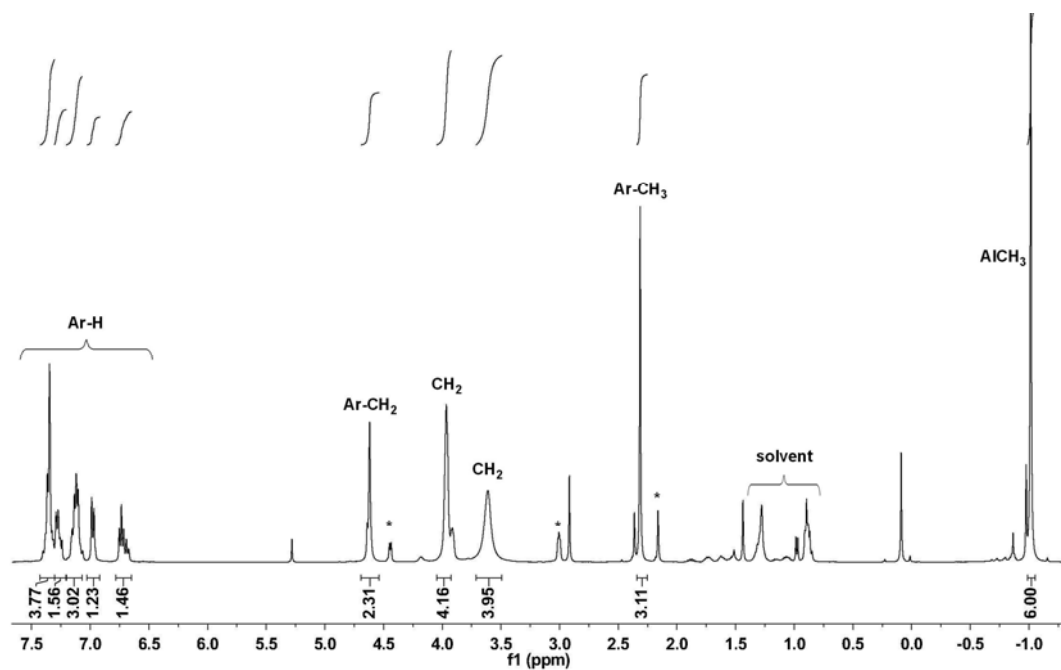


**Figure S37.**  $^1\text{H}$  NMR spectrum of complex **3g** ( $\text{CDCl}_3$ , 400 MHz). \* The free ligand formed during the course of measurement.

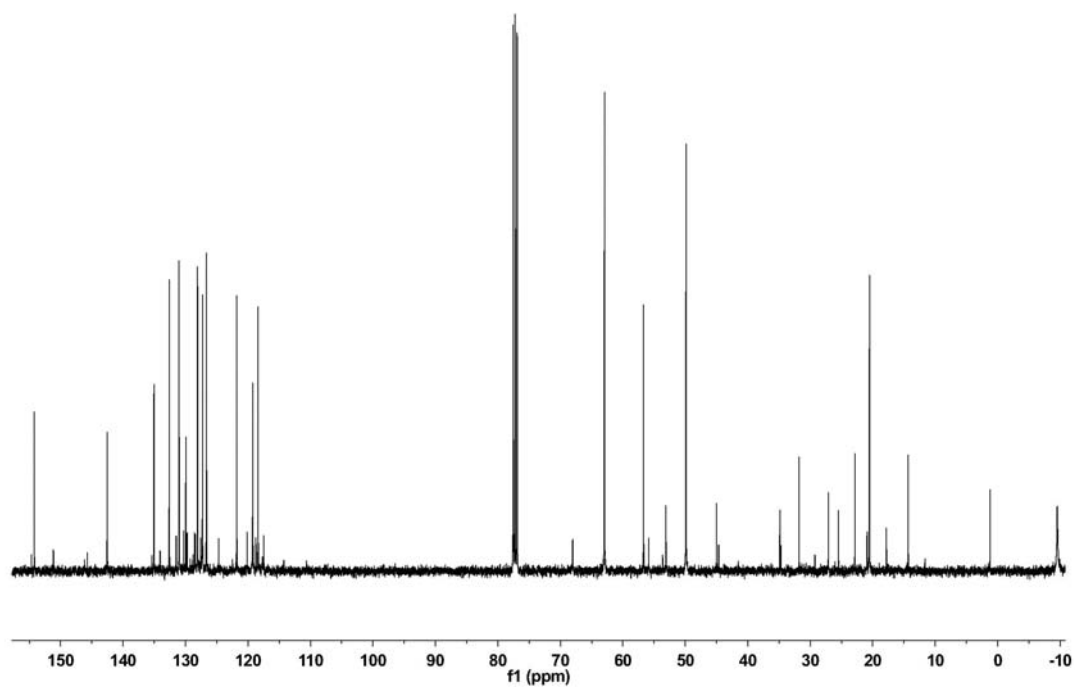


**Figure S38.** The  $^{13}\text{C}$  NMR spectrum of complex **3g** ( $\text{CDCl}_3$ , 100 MHz).

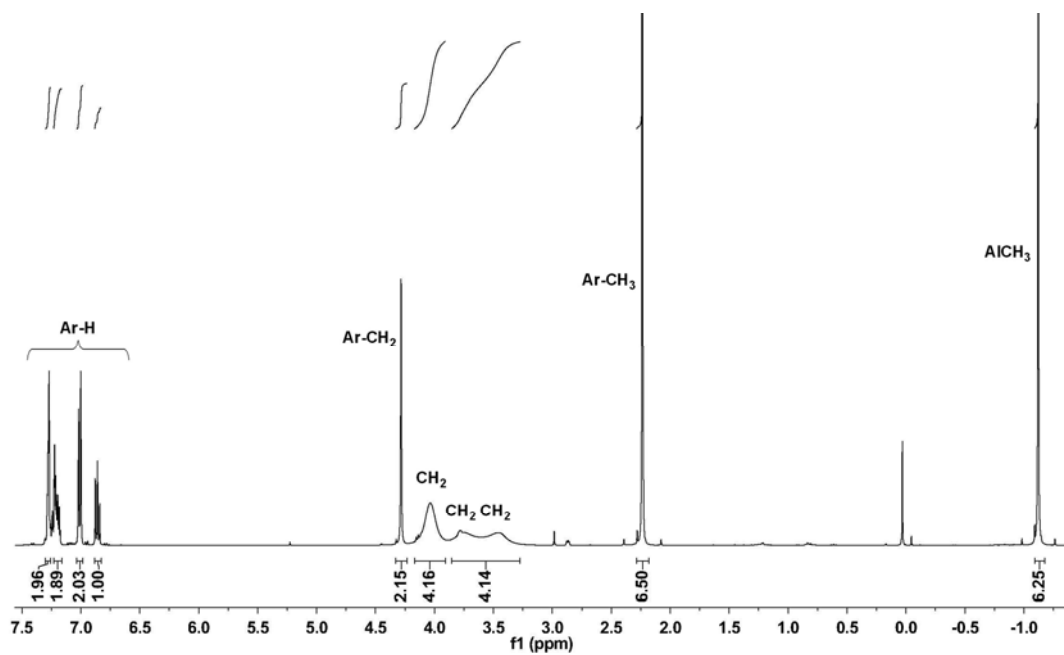


**Figure S39.** The  $^1\text{H}$  NMR spectrum of complex **3h** ( $\text{CDCl}_3$ , 400 MHz).

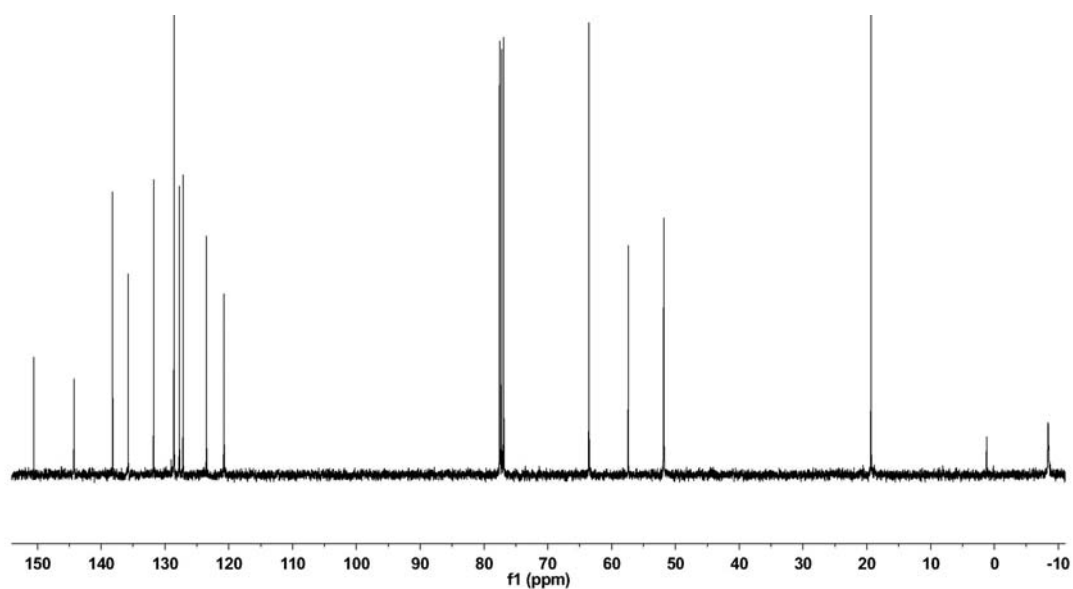


**Figure S40.** The  $^{13}\text{C}$  NMR spectrum of complex **3h** ( $\text{CDCl}_3$ , 100 MHz).

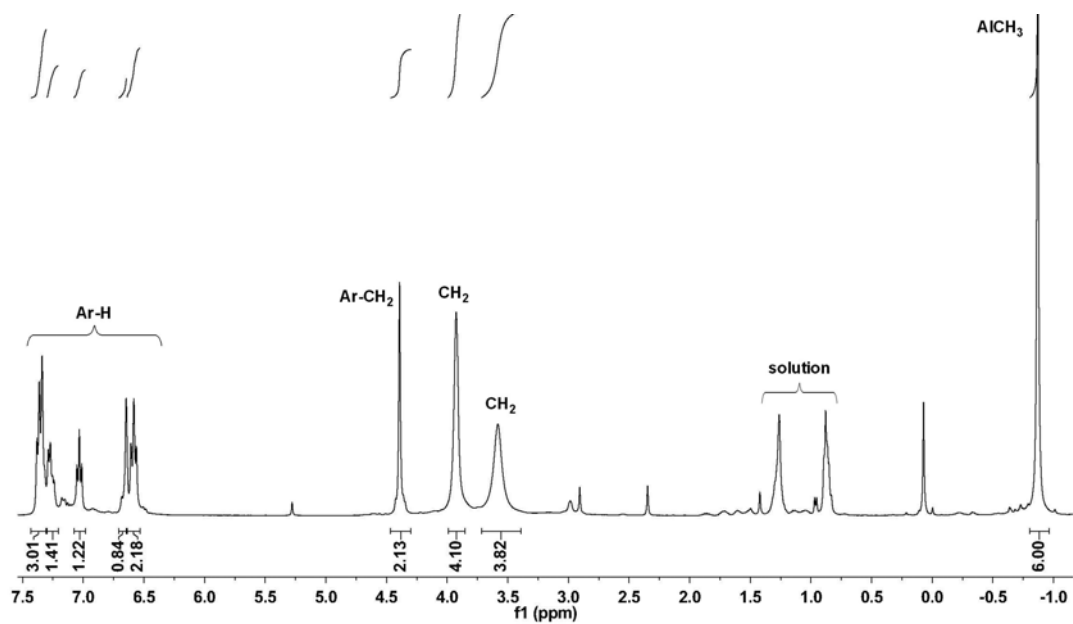


**Figure S41.** The  $^1\text{H}$  NMR spectrum of complex **3i** ( $\text{CDCl}_3$ , 400 MHz).

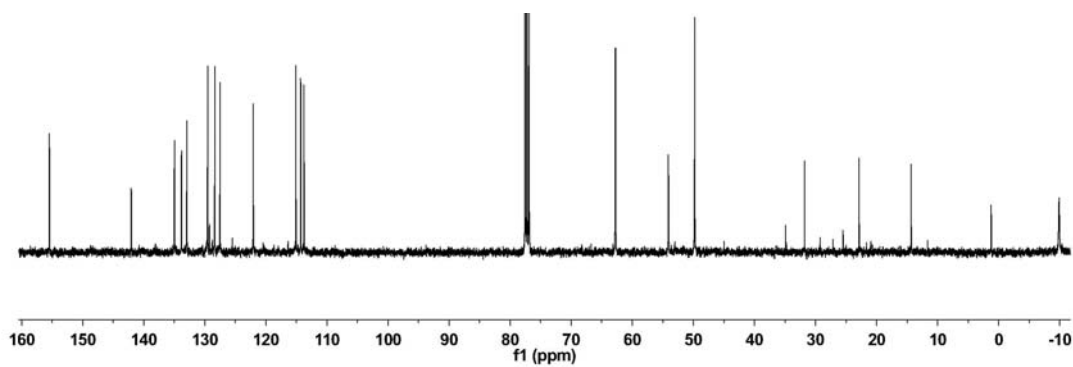


**Figure S42.** The  $^{13}\text{C}$  NMR spectrum of complex **3i** ( $\text{CDCl}_3$ , 100 MHz).

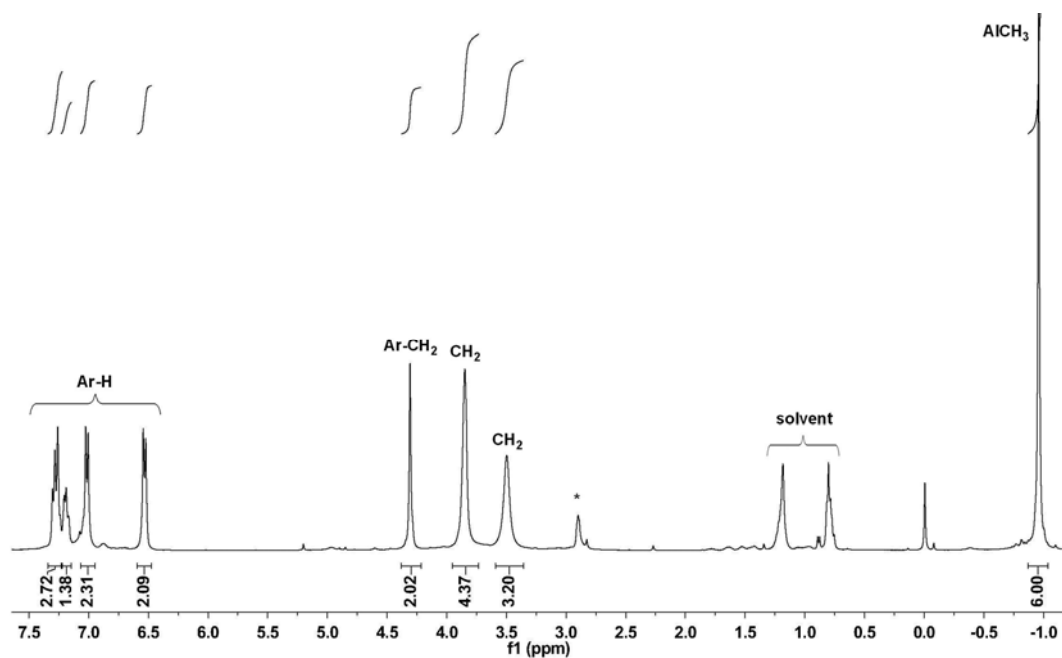


**Figure S43.** The  $^1\text{H}$  NMR spectrum of complex **3j** ( $\text{CDCl}_3$ , 400 MHz). \* The free ligand formed during the course of measurement.

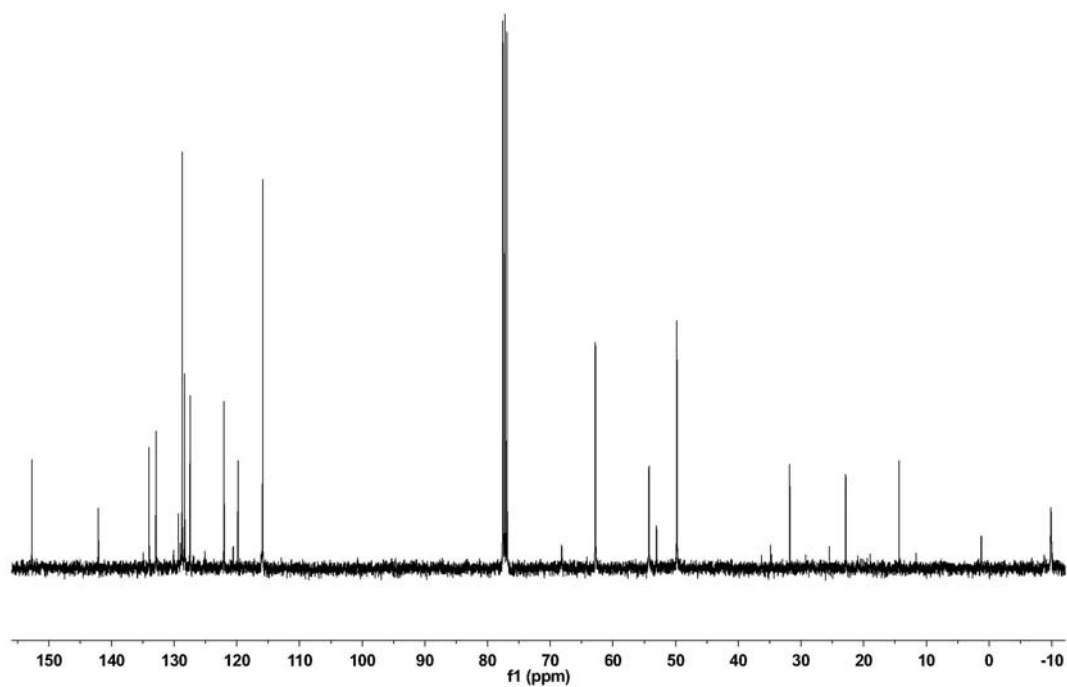


**Figure S44.** The  $^{13}\text{C}$  NMR spectrum of complex **3j** ( $\text{CDCl}_3$ , 100 MHz).



### 3. Representative GPC traces of the obtained PLA samples

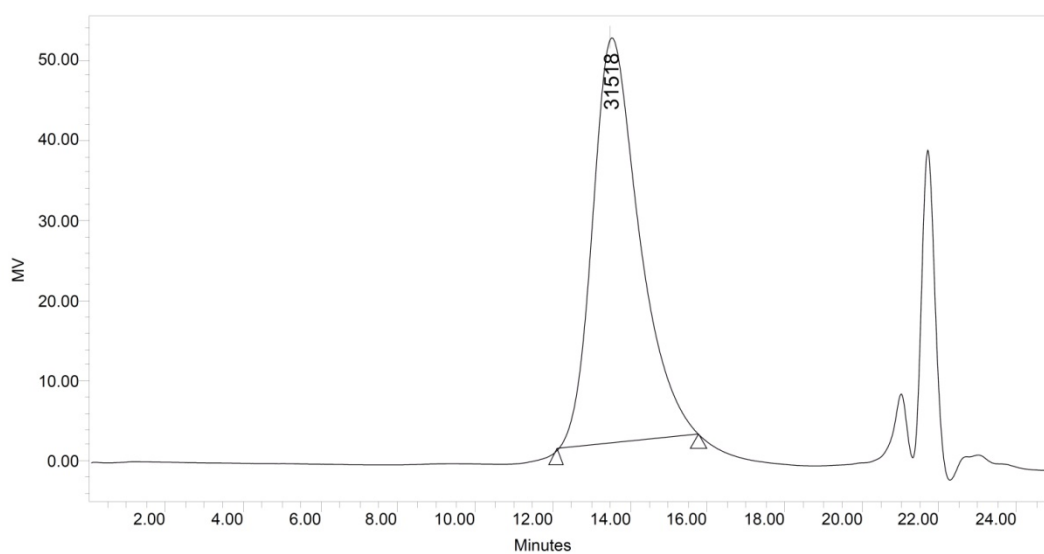


**Figure S45.** GPC trace of isolated PLA prepared via ROP of *rac*-lactide by **3f**.  
Conditions: 100 equiv. of *rac*-lactide, 65 °C, toluene, 91% conversion, 18 h.

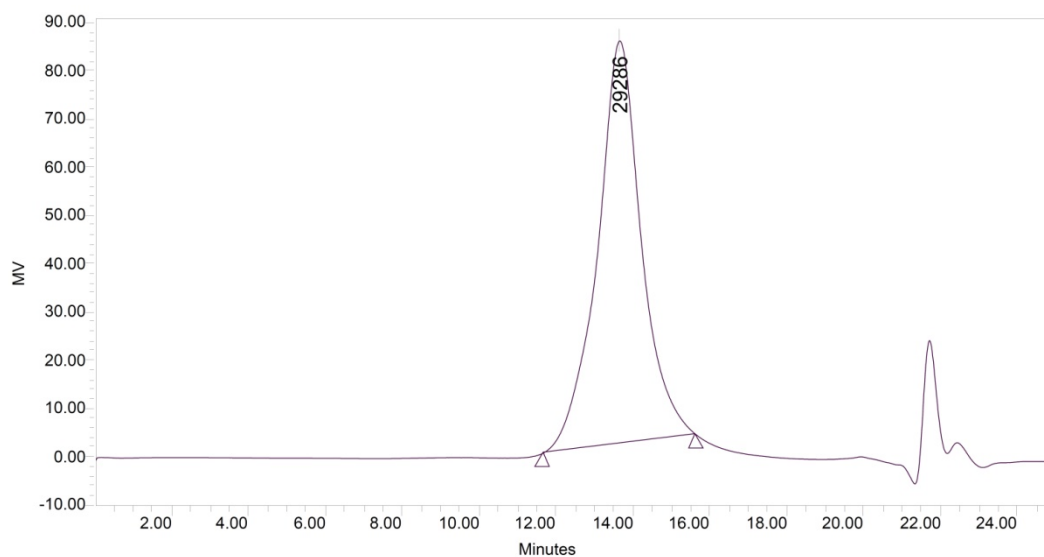


**Figure S46.** GPC trace of isolated PLA prepared via ROP of *rac*-lactide by **3c**.  
Conditions: 100 equiv. of *rac*-lactide, 65 °C, toluene, 92% conversion, 20 h.

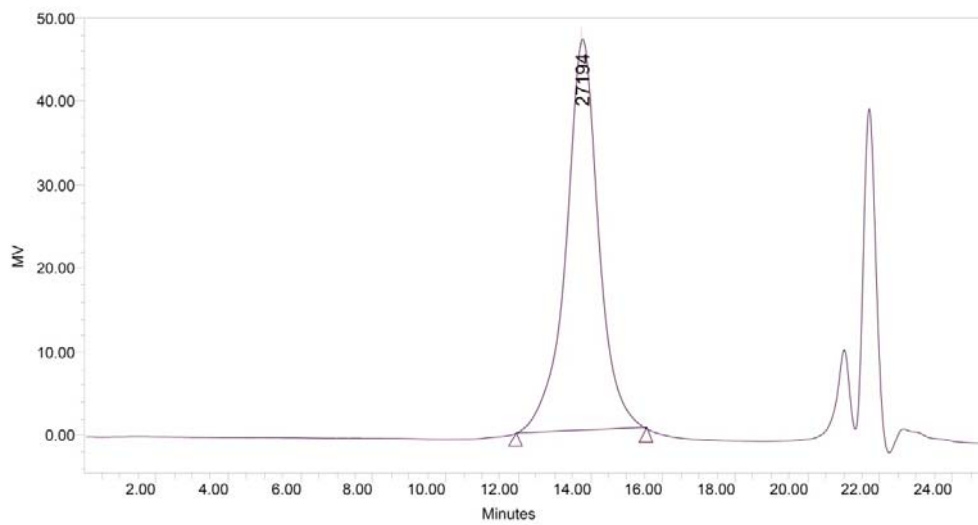


**Figure S47.** GPC trace of isolated PLA prepared via ROP of *rac*-lactide by **3e**.  
Conditions: 100 equiv. of *rac*-lactide, 65 °C, toluene, 88% conversion, 15 h.

#### 4. NMR studies of *rac*-LA oligomerization initiated by complex **3f**

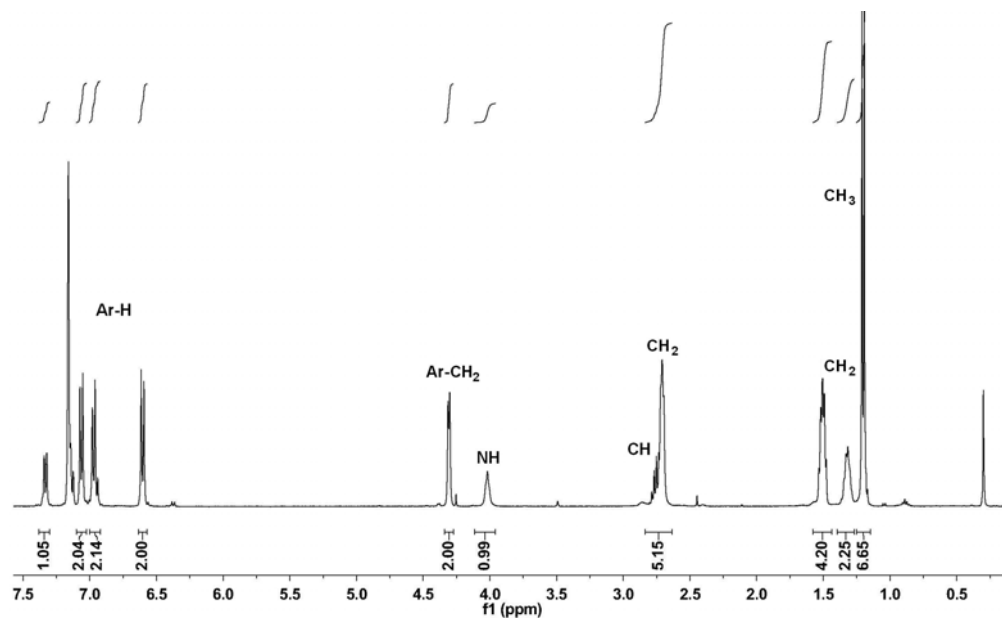


Figure S48. The  $^1\text{H}$  NMR spectrum of the ligand **1f** in  $\text{C}_6\text{D}_6$  (400 MHz).

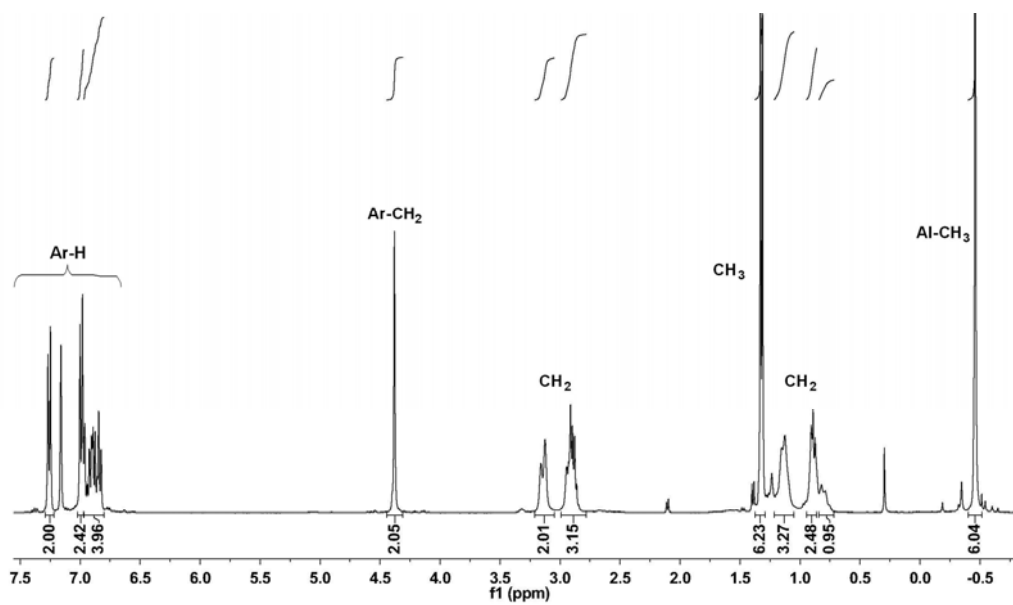
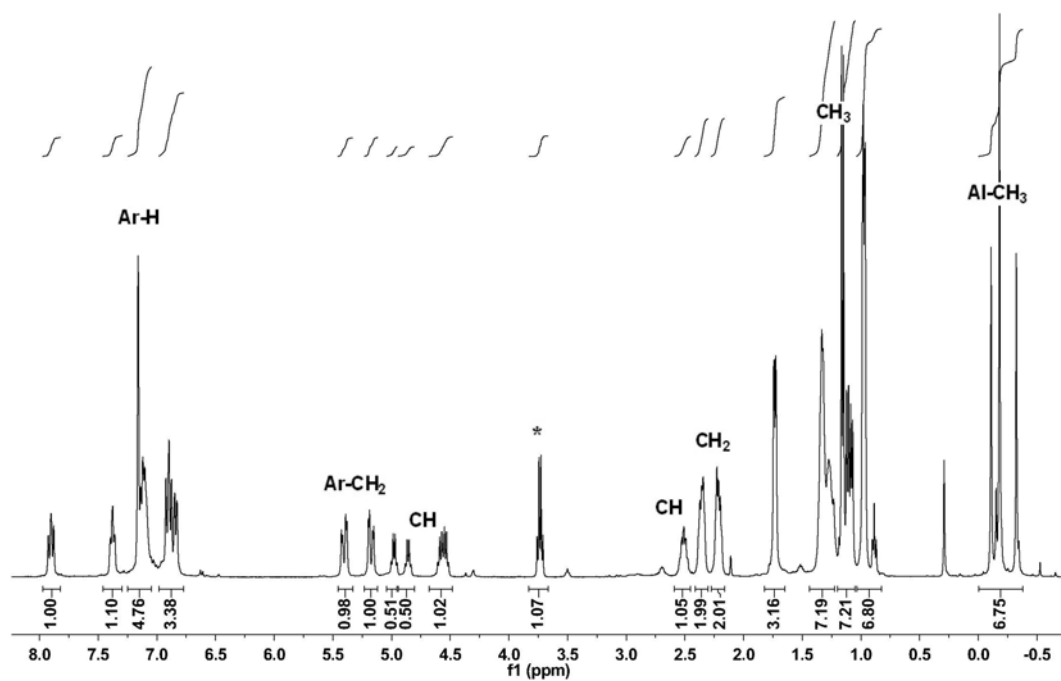
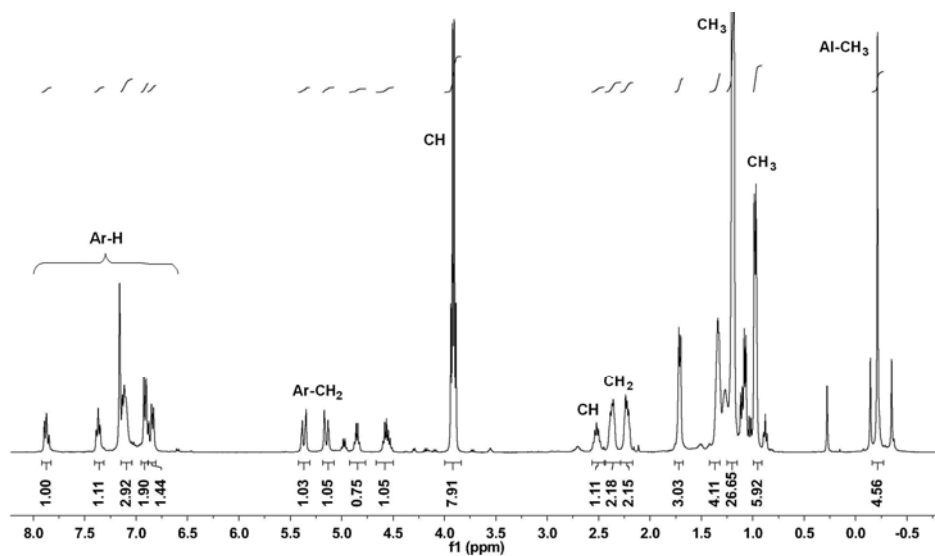


Figure S49. The  $^1\text{H}$  NMR spectrum of the complex **3f** in  $\text{C}_6\text{D}_6$  (400 MHz).



**Figure S50.** The  $^1\text{H}$  NMR spectrum of the mixture of the complex **3f** and *rac*-LA ( $[\mathbf{3f}]: [\textit{rac}\text{-LA}] = 1 : 1.5$ ) at room temperature ( $\text{C}_6\text{D}_6$ , 400 MHz; \* free lactide monomer).



**Figure S51.** The  $^1\text{H}$  NMR spectrum of the mixture of the complex **3f** and *rac*-LA ( $[\mathbf{3f}]: [\textit{rac}\text{-LA}] = 1 : 1.5$ ) at room temperature ( $\text{C}_6\text{D}_6$ , 400 MHz).

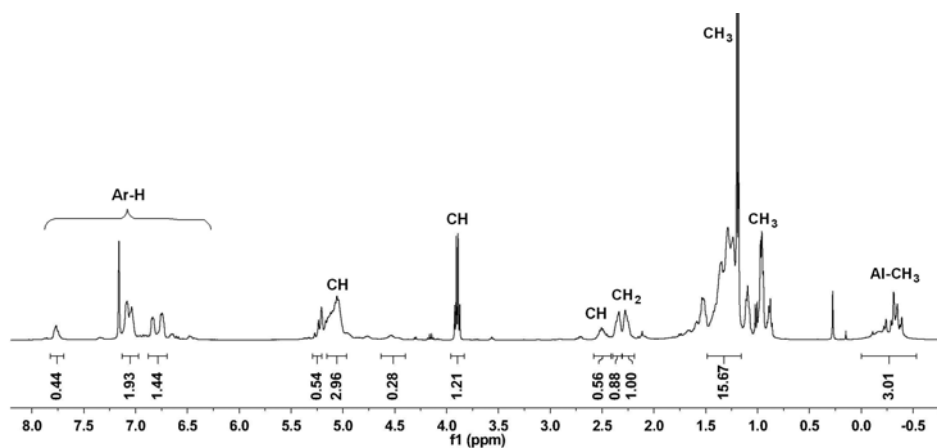


**Figure S52.** The  $^1\text{H}$  NMR spectrum of the mixture of the complex **3f** and *rac*-LA ( $[\mathbf{3f}]: [\textit{rac}\text{-LA}] = 1:5$ ) at  $65^\circ\text{C}$  after 50 min ( $\text{C}_6\text{D}_6$ , 400 MHz).

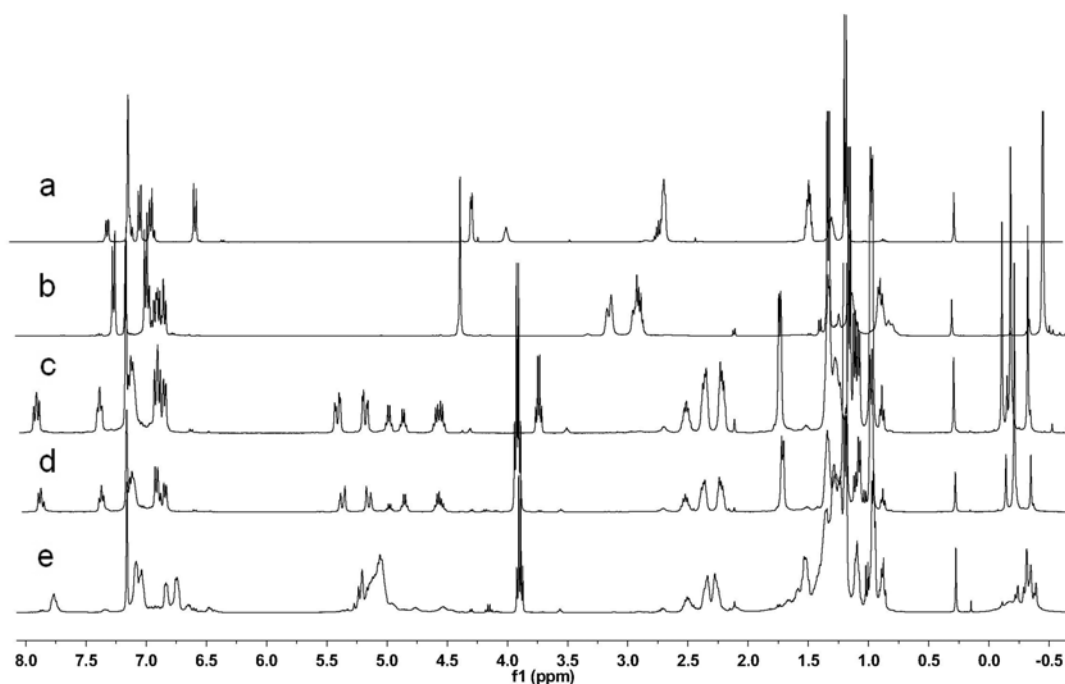


**Figure S53.** The comparison of  $^1\text{H}$  NMR spectra of (a) ligand **1f**; (b) complex **3f**; (c) the reaction mixture of complex **3f** and *rac*-LA ( $[\mathbf{3f}]: [\textit{rac}\text{-LA}] = 1:1.5$ ) at room temperature; (d) the reaction mixture of complex **3f** and *rac*-LA ( $[\mathbf{3f}]: [\textit{rac}\text{-LA}] = 1:5$ ) at room temperature; (e) the reaction mixture of the complex **3f** and *rac*-LA ( $[\mathbf{3f}]: [\textit{rac}\text{-LA}] = 1:5$ ) at  $65^\circ\text{C}$  after 50 min ( $\text{C}_6\text{D}_6$ , 400 MHz).